APPENDIX G. OPEN ROADWAY TESTS

This appendix summarizes the results of the FLAR program testing conducted on the open roadway. The open roadway tests are divided into two categories:

- Background Tests. Conducted with little or no traffic to assess the roadway background environment.
- Traffic Tests. Conducted with varying levels of traffic density.

G.1 BACKGROUND TESTS

The purpose of the background tests was to characterize the "non-traffic" component in the radar returns from common roadway objects that will appear within any forward-looking radar's field of view. The data for these tests were collected by taking the ERIM Testbed Vehicle on the roadways in the greater Ann Arbor area and identifying route segments with background attributes of interest. Data on the following types of roadway background were collected:

- Bridge Overpasses
- Different Road Types
- Guard Rails
- Roadside Signs
- Hills

A variety of data sets were collected on the roadway and analyzed using the ERIM FLAR Analysis Software. Data sets of interest were further processed using custom Matlab scripts to extract desired information from the raw radar data. The remainder of this section will summarize the results for the various background tests. Sample data plots will be used to illustrate results and diagrams provided where necessary.

G.1 .1 Bridge Overpasses

Bridge overpasses are of a particular concern to forward-looking radars because they extend over the entire roadway and, therefore, may appear as a stopped object within the primary vehicle's lane. This could occur even with radar's outfitted with the finest azimuthal resolution. Radar designers have approached this problem by limiting the antenna's beam width in the vertical plane in an effort to keep the overpass structures beyond the radar's field of view.

The TRW FLAR has a 3 dB elevation beam width of 3 degrees. The plot in Figure G-l shows the elevation plane 3 dB pattern for a 3 degree radar beam. Also, the plot includes reference lines for 12 and 14 foot bridges. Note that the beam height is 0.75 meters at a 0 meter range. This value corresponds to the mounting height of the TRW FLAR on the ERlM Testbed Vehicle.

Figure G-l shows that the 3 dB point of a 3 degree radar beam does not intersect with a 12 foot bridge until beyond a 100 meter range. This was an important factor in the selection of a 3 degree beam width in elevation. However, as the back of the vehicle is loaded with cargo, this beam pattern could be offset (i.e., tilted) up to several degrees. As the loading increases, the offset becomes more severe, and the antenna beam begins to illuminate the overpass structure. The tests described below were conducted to evaluate the extent to which an elevation offset in the radar beam would effect the returns in the raw radar data induced by bridge overpasses. These tests were conducted on US-23 under the Earhart Road bridge which is about 14 feet above the roadway.

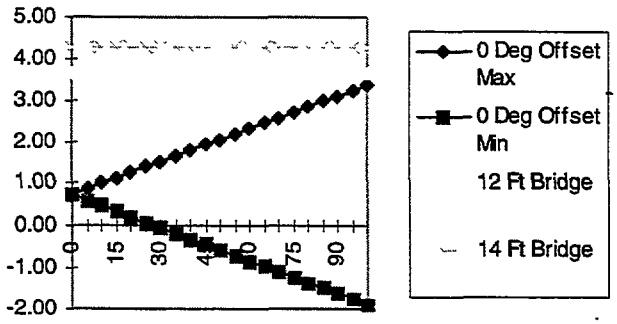

Figure G-1. Overpass Illumination—0° Offset

0 Degree Offset

Many runs under bridge overpasses have been made throughout the data collection phase of this program, and no evidence of returns from the overpass structures have been observed. As part of the bridge overpass tests, data collections were taken with a 0 degree offset under the Earhart Bridge on US-23 (14 feet above the road). A 10 dBsm corner reflector was placed on the top portion of the bridge for reference. The data was analyzed and no returns from the bridge overpass structure were observed.

1 Degree Offset

To simulate the loading of the ERIM Testbed Vehicle, the FLAR RF unit was tilted to a 1 degree offset. The plot in Figure G-2 shows the 3 dB illumination pattern for a 1 degree offset in the FLAR 3 degree antenna. Notice that the plot indicates an intersection of the beam pattern with the 14 foot bridge at about 80 meters. Therefore, one could expect that returns from the bridge overpass structure would be observable when the range to the bridge is between 80 and 100 meters.

Figure G-3 is the actual raw radar data collected during the test run. The returns from the bridge overpass structure are annotated on the plot. The returns from the overpass structure are observable from the time the bridge is 100 meters from the radar until it is nearly 60 meters from the radar. The reason the overpass was observed all the way down to 60 meters instead of being lost at 80 meters as depicted in Figure G-2 is that the plot in Figure G-2 is the illumination pattern for the 3 dB point on the antenna beam. The actual antenna beam provides gain (at a much lower level) beyond the 3 dB point and therefore, illuminates the bridge.

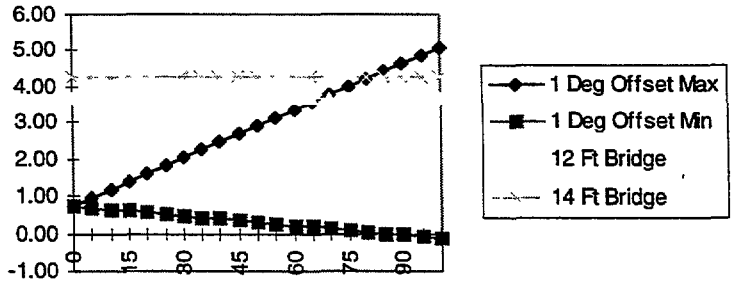

Figure G-2. Overpass Illumination—1° Offset

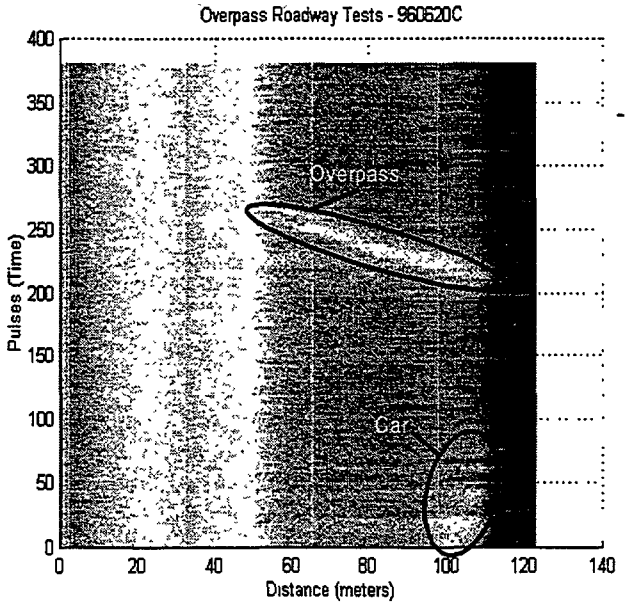

Figure G-3. Overpass Returns—1° Offset

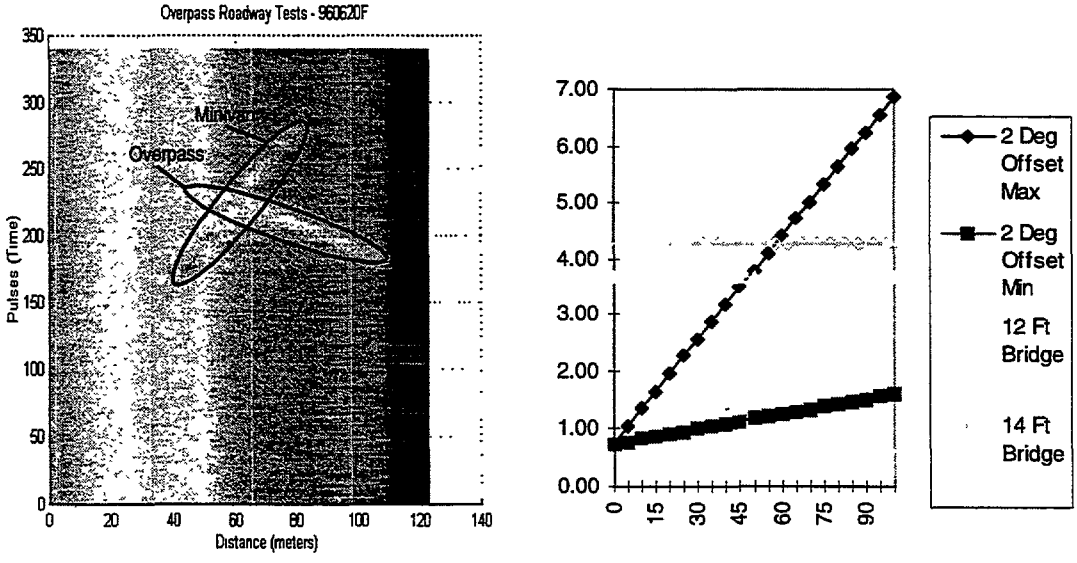

Figure G-4. 2 Degree Offset Data

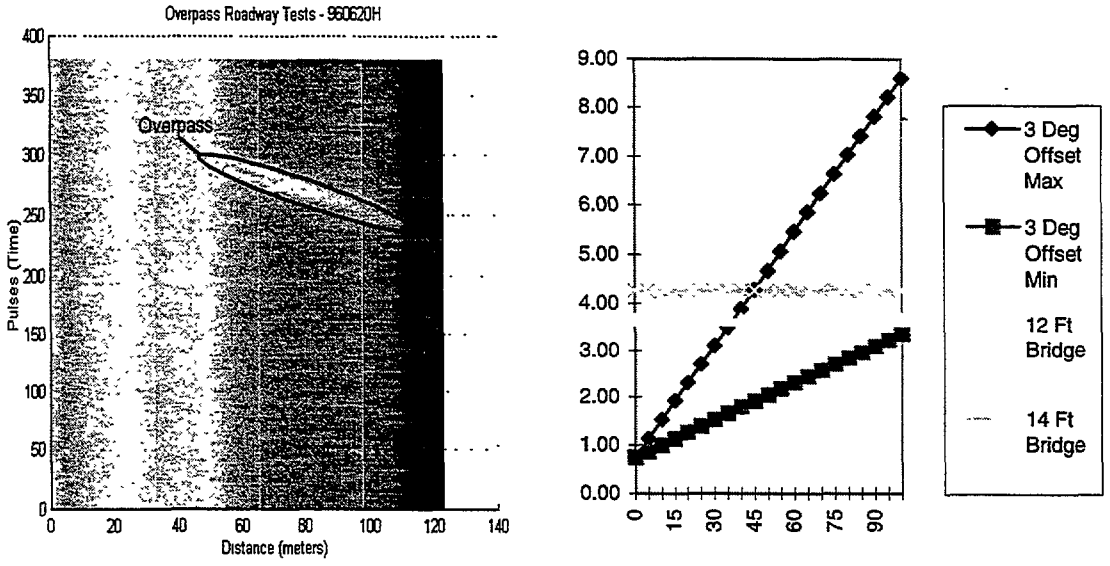

Figure G-5. 3 Degree Offset Data

2 and 3 Degree Offset

Test runs were made with the FLAR's angle of inclination at 2 and 3 degrees. The raw radar data and 3 dB antenna illumination plots corresponding to the 2 and 3 degree offset runs are shown in Figures G-4 and G-5, respectively. As the offset angle increases, the returns from the bridge overpass structure are observable at progressively nearer ranges. The raw radar data plot in Figure G-4 includes returns from a mini-van which was in the FLAR's field of view at the same time the bridge overpass returns were present.

It is interesting to note that in these test the FLAR, utilizing TRW-proprietary algorithms, did NOT lock-on and track the returns from the bridge overpasses. The FLAR did, however, briefly track the mini-van during the 2 degree offset test.

During the 2 and 3 degree offset tests, the maximum exhibited RCS value was -1 dBsm. It was determined that the 10 dBsm corner reflector placed on the TOP portion of the bridge structure was NOT contributing to the returns for these tests.

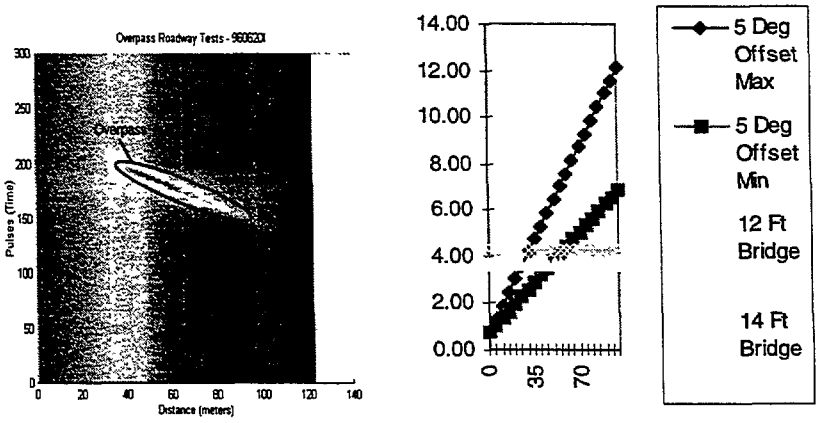

Figure G-6. 5 Degree Offset Data

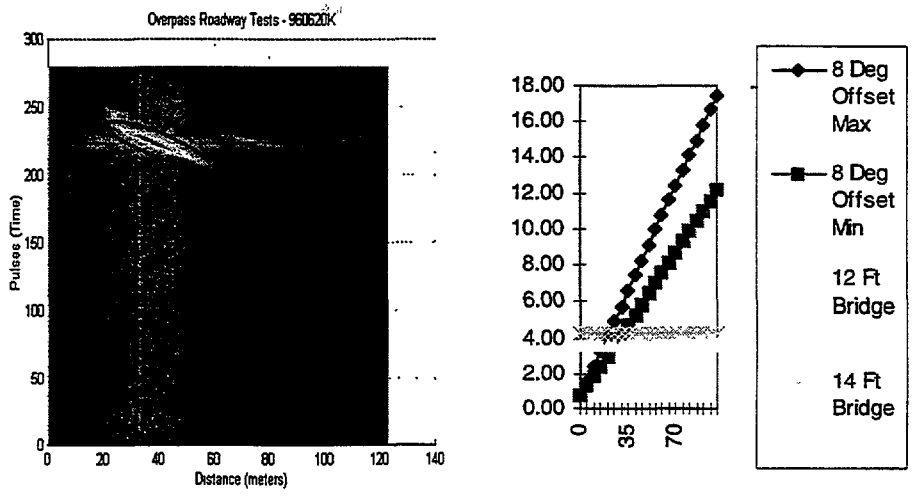

Figure G-7. 8 Degree Offset Data

5 and 8 Degree Offset

The raw radar data and illumination plots for the 5 and 8 degree offset tests are provided in Figures G-6 and G-7, respectively. As expected, the returns from the overpass structure increased in amplitude as the offset angle increased. The maximum exhibited RCS from the overpass structure was about 5 dBsm for the 8 degree offset collection. The 10 dBsm corner reflector which was placed at the top of the overpass structure was removed and subsequent collections were made to verify that the corner reflector was NOT contributing to the measured RCS values.

Suprisingly, the FLAR did not lock on and track the overpass structure returns in any of the tests. Without detailed knowledge of the TRW-proprietary algorithms within the FLAR unit, it is difficult to specify the exact reason that the FLAR seemed to ignore the overpass returns. However, since the FLAR was designed for ACC applications, and not collision avoidance, the threat assessment/tracking algorithm may have discarded the overpass returns based on their relative range rate and transient appearance in the raw data.

The 5 and 8 degree offset tests were seen to differ from the 1, 2, and 3 degree tests in that returns from the overpass structure were not observed until a range well under 100 meters. This is due to the beam illumination patterns as illustrated in Figures G-6 and G-7. Because of the elevation angle offset, the lower extent of the illumination pattern does not illuminate the overpass until ranges well under 100 meters.

Bridge Overpass Conclusions

The bridge overpass tests indicated that even a slight 1 degree change in the elevation angle of the FLAR resulted in the detection of overpass returns in the raw radar data. As this elevation offset angle is increased, the return levels from the overpass also increased. The table below summarizes the maximum RCS exhibited by the overpass structure for a given elevation offset angle.

Table G-1. Overpass RCS

Elevation Angle Offset	Maximum Overpass RCS
0 degrees	No returns
1 degree	-10 dBsm
2 degrees	-8 dBsm
3 degrees	-1 dBsm
5 degrees	2.5 dBsm
8 degrees	7 dBsm

The fact that the FLAR did not track (i.e., report) the range to the bridge overpass indicates that the ACC application optimized algorithms within the FLAR may not perform well for collision warning applications.

G.1.2 Road Types

The FLAR sensor was exposed to a number of different road types during the data collection phase of this program. These road types included concrete, asphalt and dirt roads. The tests described here were conducted to evaluate the effects of the various roadways on radar response as a result of returns produced by reflections from the roadway itself. The results from the "Road Type" tests are summarized in Figure G-8.

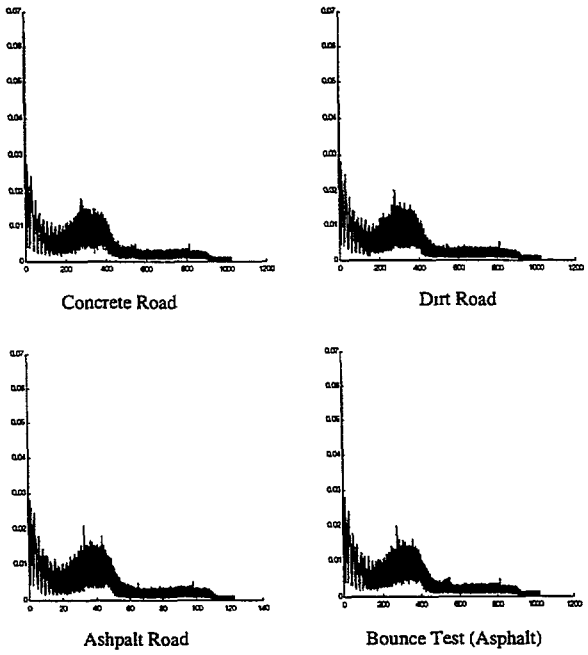

Figure G-8. Returns From Various Road Surfaces

The plots in Figure G-8 are range profile plots taken over several hundred radar pulses. The data was collected with the ERIM Testbed Vehicle moving down a road segment with no other targets within the radar field of view. The issue with the various road types was whether or not their relative roughness

would induce different responses in the radar sensor. As illustrated in Figure G-1, the 3 degree elevation beam width of the FLAR radar intersects with the ground at about 30 meters. Analyzing the data in the plots indicates that there are no significant changes in radar returns resulting from the type of roadway.

The "hump" in the range profiles which appears from 20 to 50 meters was initially thought to be caused by returns from the intersection with the ground surface. A "bounce test" was conducted (see plot 4 in Figure G-8) in which the front portion of the vehicle was bounced up and down in an attempt to change the hump's profile. However, as seen, the bounce tests had no effect on the characteristic hump. The hump and nearer range return levels are part of the baseline operating characteristics of the FLAR sensor. See section 4 in the body of the report for further discussion of baseline performance characteristics.

The conclusion from these tests is that the returns from the radar beam illumination of the ground surface is insignificant with respect to the noise floor of the FLAR sensor. Even the very bumpy dirt road used in these tests failed to produce any observable changes in radar response.

One other issue which deserves further study is the difference in multipath effects which are due to various road surfaces. Surface moisture should also be included in further studies. Evidence of multipath off the road surface were observed on several occasions during the road testing. Multipath off of the roadway surface can actually allow the transmitted radar energy to pass under a preceding vehicle. Furthermore, this energy can be reflected off of objects in front of a preceding vehicle, allowing the radar to "see" objects not in its direct field of view.

G.1.3 Guard Rails, Signs, and Hills

Figure G-9 shows raw radar returns collected during some S-curve maneuvers on a 2-lane roadway. The returns in the plot were induced by guard rail and metal sign posts located on the roadway. The guard rail resulted in a much more significant return than the signs. A detailed description of guard rail return characteristics is provided in Section 10 of Appendix F.

The return levels induced by the signs were generally found to exhibit an RCS characteristic level somewhere between 0 and 3 dBsm. For the roadway dynamics corresponding to the data in Figure G-9, the radar returns from the signs were very transient and had a very high range rate associated with them.

The FLAR and its TRW-proprietary algorithms did not report on (i.e., track) any of the road signs encountered during the roadway tests.

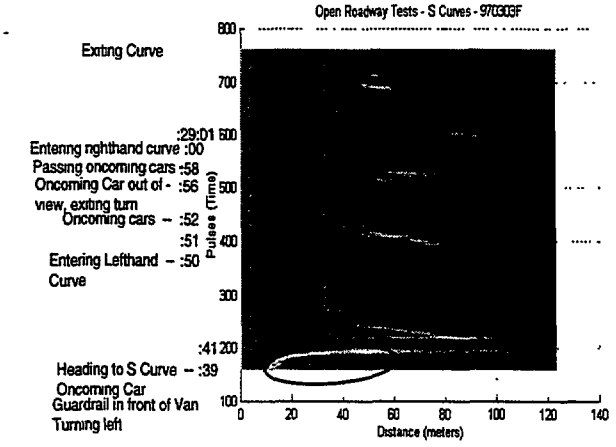

Figure G-9. Returns on Curved Roadway

Similar to the various roadway type tests described previously, the hill tests conducted on various roadway showed no signs of significant radar response due to the hill itself. The effect the hills did have on the radar sensor were all related to loss of track on target vehicles as they departed from the radar's field-of-view due to passing over a hill in the roadway. Again, the hills themselves did not induce any response in the radar.

G.1.4 Traffic Tests

The traffic tests conducted under this program were aimed at qualitatively evaluating the open roadway environment. On the open roadway, a forward looking radar is exposed to numerous types of objects with diverse dynamic characteristics. The object-rich environment in which the radar must operate consists of other moving vehicles and roadside "stuff". We have categorized this "stuff" as background objects. These background objects include bridge overpasses, signs, guard rails, and so forth. The response to these background types of objects has been discussed previously. This section will focus on qualitatively examining the returns from other moving vehicles. The following three areas will be addressed in this section:

- Complexity of Road Environment
- On-coming Traffic Characteristics
- "Non-standard" Vehicles

G.1.5 Complexity of Roadway Environment

To evaluate the FLAR response to other moving vehicles, a number of collections were made in various traffic densities. While higher traffic densities would seem to constitute a much more difficult environment for the FLAR, it is important to remember that the sensor's field of view limits the number of targets which generate returns to the radar. Figure G-10 illustrates how the radar's FOV limits the number of objects which can be tracked. The lightly shaped target in the left lane of Figure G-10 will not cause a return to be induced in the radar. This indicates that the traffic density present outside of the radar's FOV has little effect on its performance.

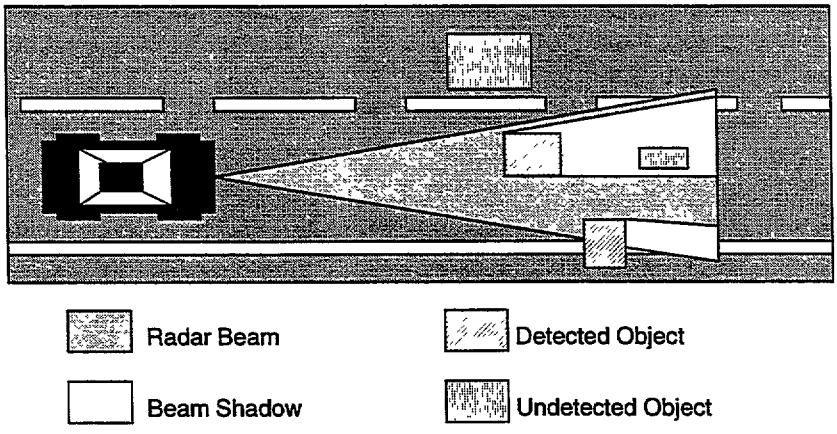

Figure G-10. FOV and Occlusion Limitations

Another factor related to the FLAR's performance in various levels of traffic density is occlusion of the radar energy. Referring to Figure G-10, one can see that the object within the host vehicle's lane and furthest in range does not induce a return to the radar because the radar energy has been occluded (blocked) by another object. (It is important to note that under certain geometries and roadway

configurations that the FLAR can actually see vehicles beyond a preceding vehicle due to multipath effects of the radar energy under the preceding vehicle.)

These two factors, sensor FOV and energy occlusion, result in the FLAR performance being less sensitive to traffic density than one might intuitively expect. The largest impact of traffic density on the FLAR performance is related to the dynamic movements between the FLAR host-vehicle and surrounding vehicles.

Figure G-l 1 illustrates the FLAR performance in a heavy traffic scenario. The text along the left side of Figure G-l 1 describes the various vehicle movements and locations along the collection timeline. Two general observations, both fairly intuitive, were made during the roadway tests with varying traffic densities:

1. As traffic density increased from light (2 to 3 cars within 100 meter stretch of road) to moderate, significantly less of the background returns were observed in the radar output. The returns which were observed were almost always from another moving vehicle.
2. As traffic density increased from moderate to heavy, similar types of returns were observed but at increasingly nearer ranges.

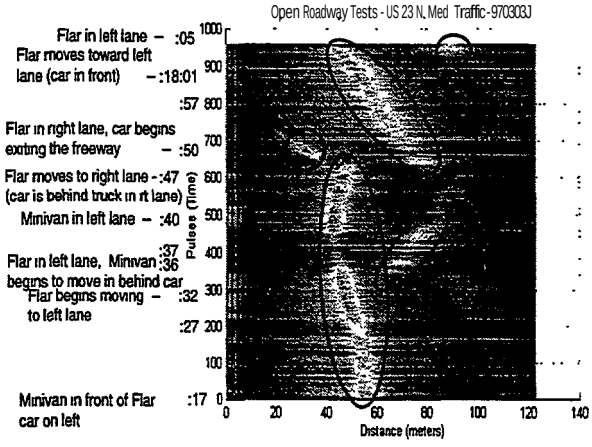

Figure G-l 1. Collection in Heavy Traffic

The first observation may actually result in the moderate traffic density scenario being easier for the threat assessment algorithm to handle than the light traffic scenario. This is due to the fact that many of the "extraneous" returns from background objects, which have high motion dynamics relative to the host vehicle, are not evident in the raw radar returns. There are reasons the background returns are no longer observable in the raw radar data. The first reason is that the increased number of vehicles are occluding the background objects. The second reason is that the returns from the vehicles (i.e., their RCS) is generally higher than that of the background objects. The automatic gain control of the FLAR is adjusted to avoid saturation from the vehicle returns, thereby reducing the sensitivity of the FLAR receiver. Therefore, the relatively weaker returns from the background objects are no longer observable.

The second observation indicates that under heavy traffic scenarios, the threat assessment algorithm has much less time to warn the operator of a potential impending crash. In addition to having less time, the algorithm may also have much less data. Due to the rapid detection and loss of track on the surrounding vehicles due to dynamic movements (see Figure G-l l), the threat assessment algorithm may end-up with significantly less of a time-location profile (i.e., track) of an object under heavy traffic conditions.

In conclusion, qualitatively speaking from a pure sensor perspective, traffic density does not have as much of an effect on sensor performance as one may intuitively expect. Field-of-view and occlusion effects play significant roles in limiting the number of returns to the radar sensor regardless of traffic density. It is important to note that their are secondary effects of higher traffic density such as multipath which can induce returns in the sensor. From a collision avoidance or ACC application perspective, the biggest impact traffic density has is related to the average time a threat assessment algorithm has to react to a particular scenario. By definition, the spacing between vehicles in high density traffic is lower and therefore reaction times are decreased.

G.1.6 Oncoming Traffic Characteristics

Several data collections were made while on a a-lane, non-divided highway on which oncoming traffic was present. The raw radar data plot in Figure G-12 summarizes how the returns from oncoming traffic manifests itself with respect to the radar sensor. The specific returns from the oncoming traffic are annotated in the figure. These returns are very transient in nature and while there are clearly evident above the sensor's noise floor, they are relatively low (on the order of -10 to -2 dBsm) when compared to typical returns from a preceding vehicle located in the host vehicle's lane.

The reason for the lower return levels is that the orientation between the radar and the oncoming vehicle is such that the vehicle is located at the edge of the radar antenna pattern. This data was collected on a straight roadway and the results are similar to those for the test track experiments conducted with a vehicle located at the side of the roadway.

This traffic scenario may cause large problems for an automotive radar designed for collision warning/avoidance. The problem is that the vehicle has a high closing rate and appears to be located within the host vehicle's lane. The high closing rate is evident in Figure G-12 by the wide almost horizontal return lines from the oncoming traffic. Also evident in the figure is that the oncoming vehicle exits the sensor's field of view at around 40 meters. Note that the FLAR's FOV for these tests was based on a 3dB beamwidth of 3 degrees. At 40 meters, an object closing at 100 MPH (assuming 50 MPH for each vehicle) has less than 1 second to impact.

The parameters of the threat assessment and warning algorithms must be set such that the false alarms from oncoming traffic is minimized. In the case of on-coming traffic on a straight-away, this would mean that the warning time would have to be set to less than 1 second, or the processing algorithms may chose to ignore oncoming traffic based on the relative speeds of the objects. Obviously ignoring objects which are approaching the host vehicle at speeds greater than its own ground speed would minimize false alarms, but would also have an impact on the number of crashes the system would be effective in mitigating.

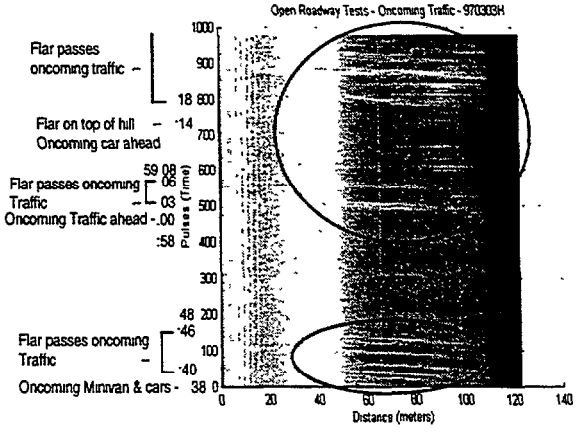

Figure G-12. Returns From On-Coming Traffic

G.1.7 Non-Standard Vehicles

Another issue regarding the data collected on the open roadway is related to the variety of vehicles on may encounter. These types of vehicles range from small sports cars, to large tractor trailers, to towed home-made wood trailers, to towed fiberglass boats, and so on. The point is that one encounters a large number of "non-standard" vehicles on the roadway.

Figure G-13 shows the FLAR radar returns resulting from following an empty automobile carrier vehicle. This vehicle is irregularly shaped and constructed primarily from metal. The plot in Figure G-13 shows how the return signature from the single vehicle is range dependent. At near ranges, there appears to be individual scattering centers located at the rear of the vehicle along with another set of scatterers towards the front of the vehicle. This second set of scatterers is located somewhere within the carrier trailer. As the range to the vehicle increases, the return from the vehicle changes in that the returns from the second set of scatterers fades away and the individual scattering centers from the rear of the vehicle blend together.

This empirical data does not indicate that the car carrier would cause any particular problems to the FLAR in terms of detection and tracking of the vehicle. However, if a FLAR implementation and processing begins to rely on particular vehicle signatures for classification or performs some sort of centroid processing to locate and track targets, these "non-standard" returns from the carrier vehicle may pose problems.

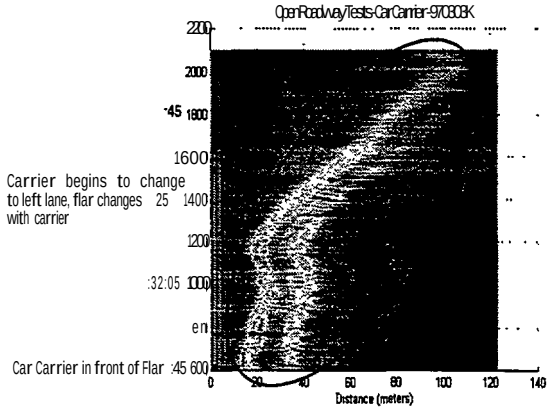

Figure G-l 3. Returns From Car Carrier Vehicle

OPEN ROADWAY DATA PLOTS

The following pages are selected raw data plots generated from the Open Roadway collections. These plots were selected to provide a reasonably sample of the type of data collected on the open road. Each plot is labeled with the appropriate test identification and annotation on the plots is provided where appropriate along with a description of the roadway environment. The reader is referred to the test results descriptions in Appendix G.

These plots are provided to assist developers in quantitatively assessing the radar response to the scenarios tested. Of course these results are specific to the TRW FLAR sensor configuration (e.g. antenna gain and beam shape). The reader is referred to Section 4 of the final report which discusses the FLAR sensor characteristics in order to extrapolate the results to other configurations.

960620 - Overpass Roadway Tests

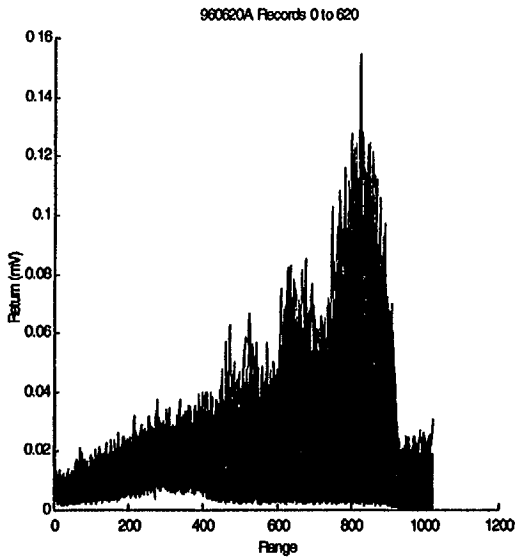

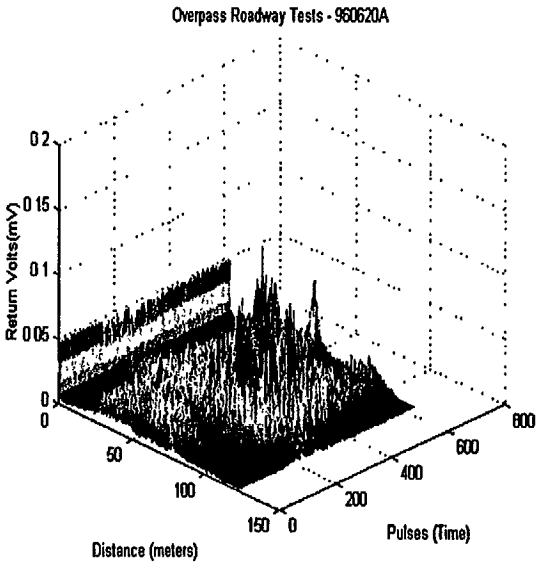

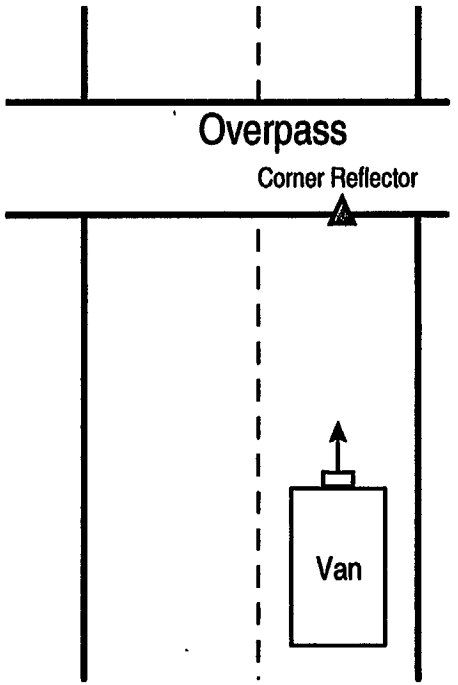

09:20:16 - Begin File
0 degree offset

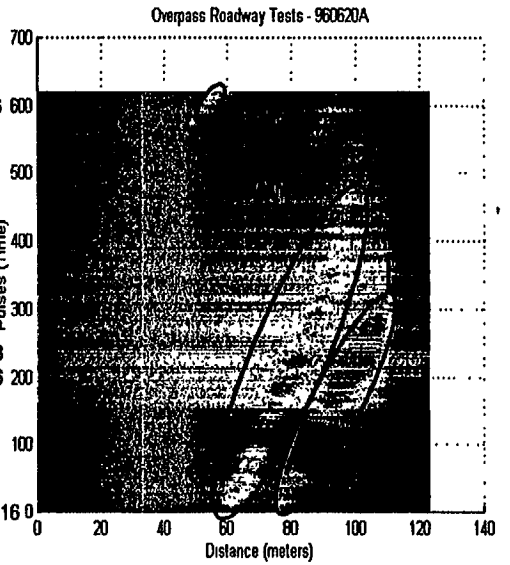

960620 - Overpass Roadway Tests

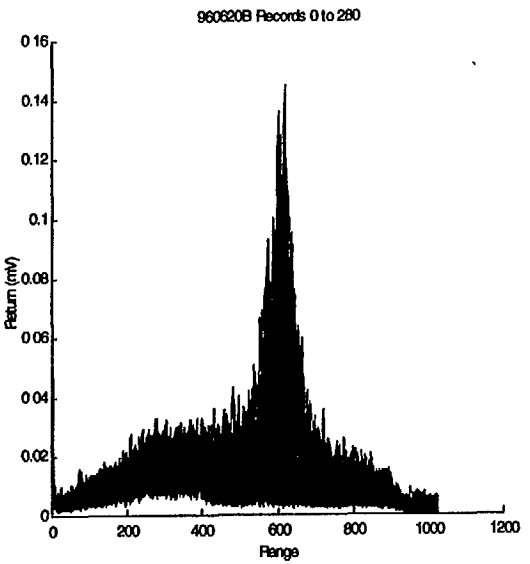

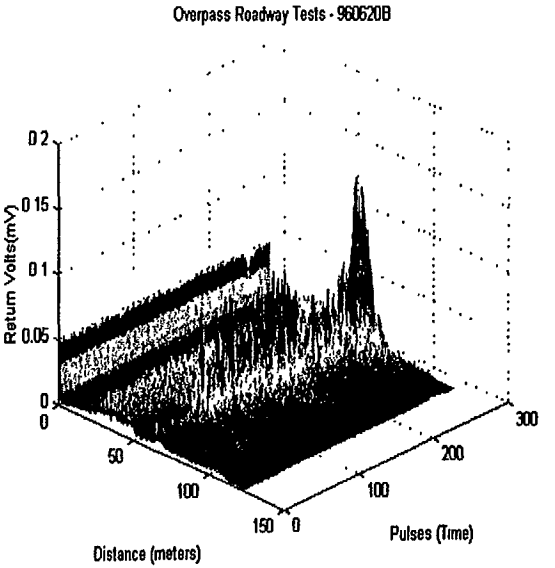

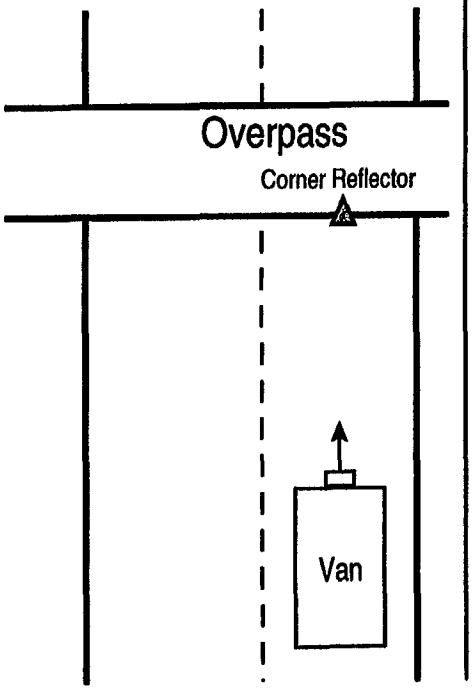

09:28:17 - Begin File
0 degree offset

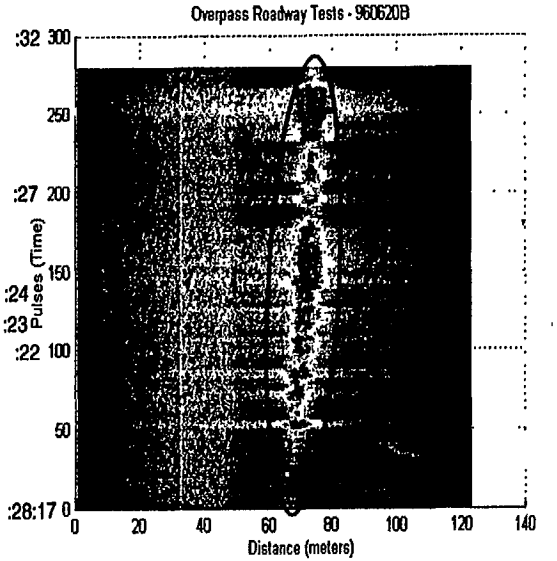

Overpass out of view -- :24
Corner out of view -- :23
Car in front of Van -- :28:17

960620 - Overpass Roadway Tests

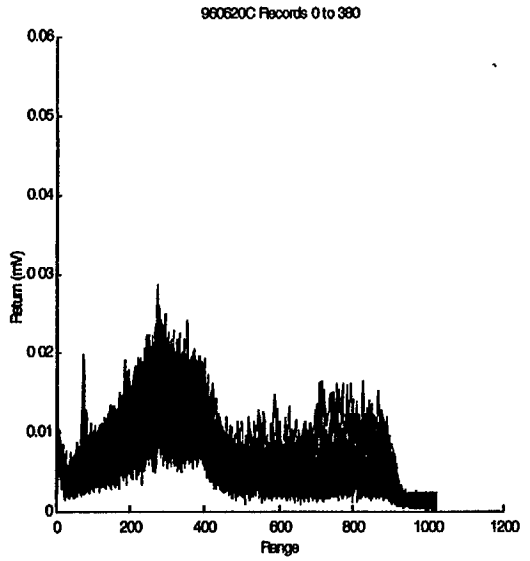

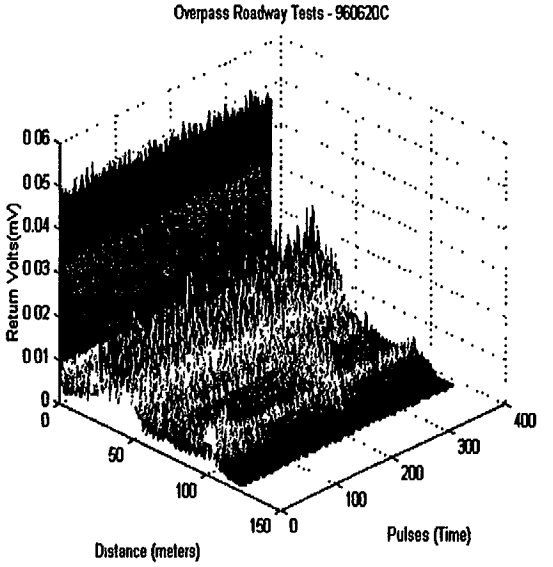

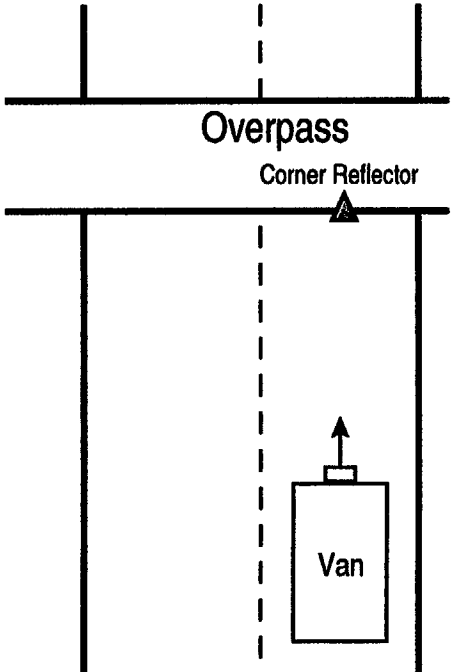

09:36:18 - Begin File
1 degree offset

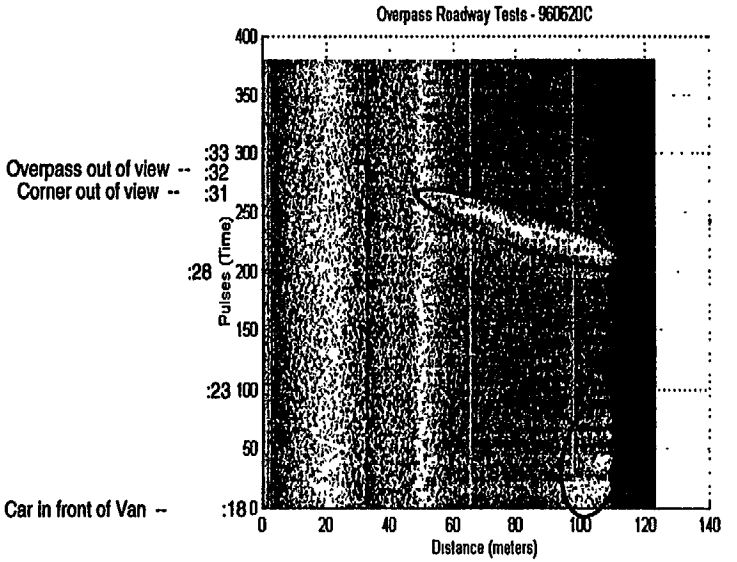

960620 - Overpass Roadway Tests

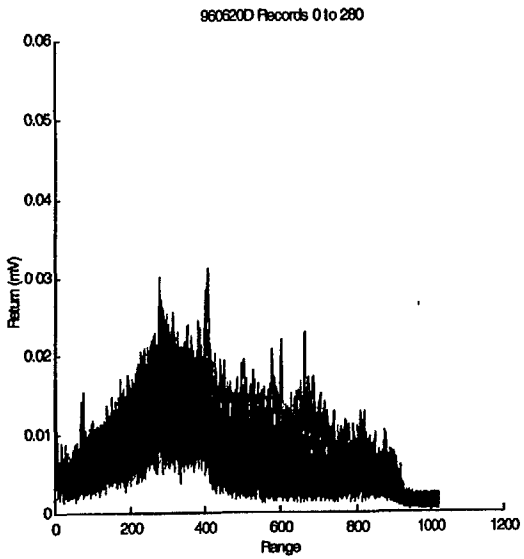

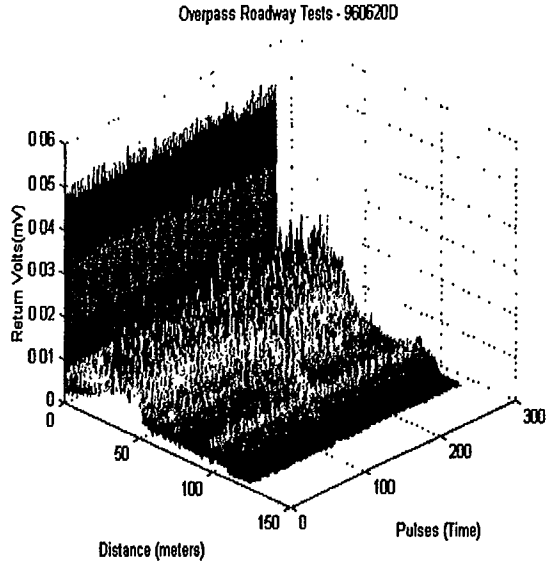

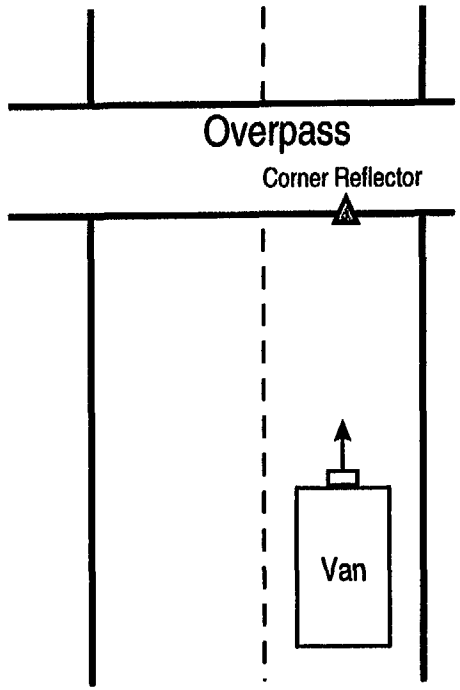

09:40:51 - Begin File
1 degree offset

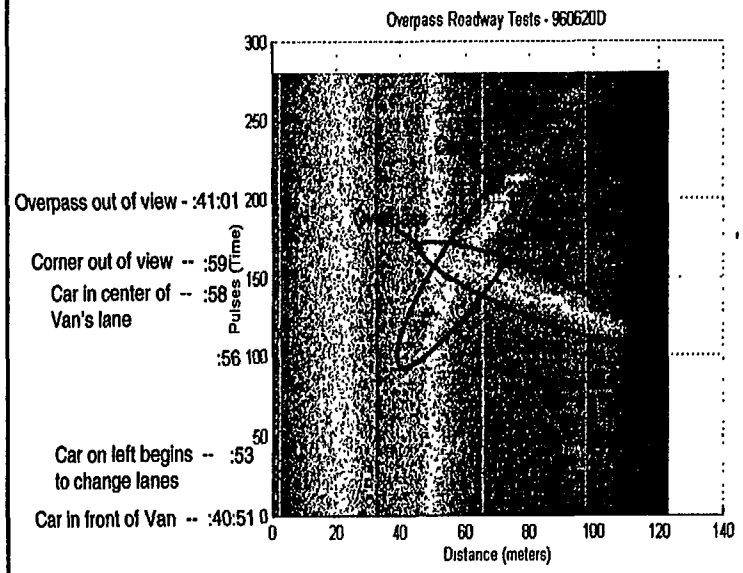

960620 - Overpass Roadway Tests

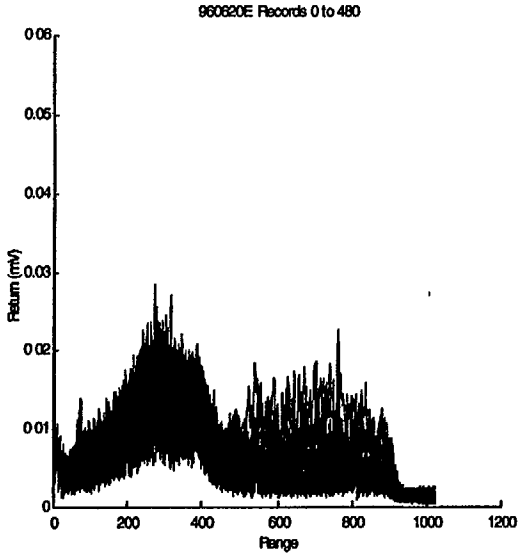

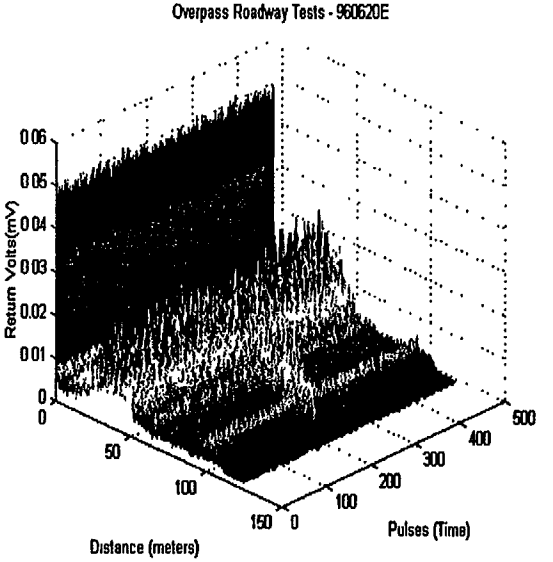

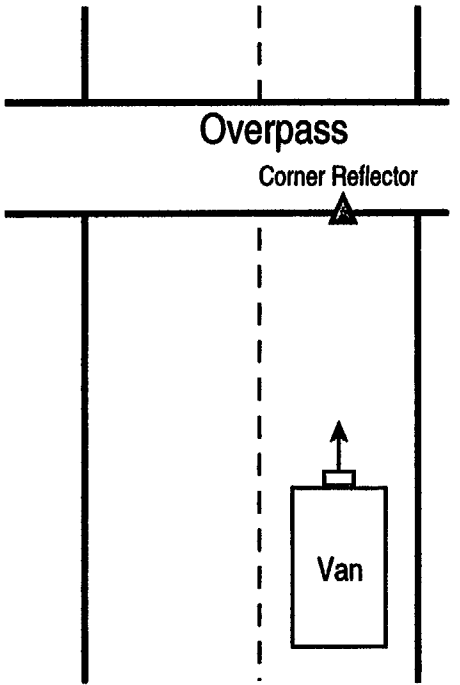

09:50:16 - Begin File
2 degree offset

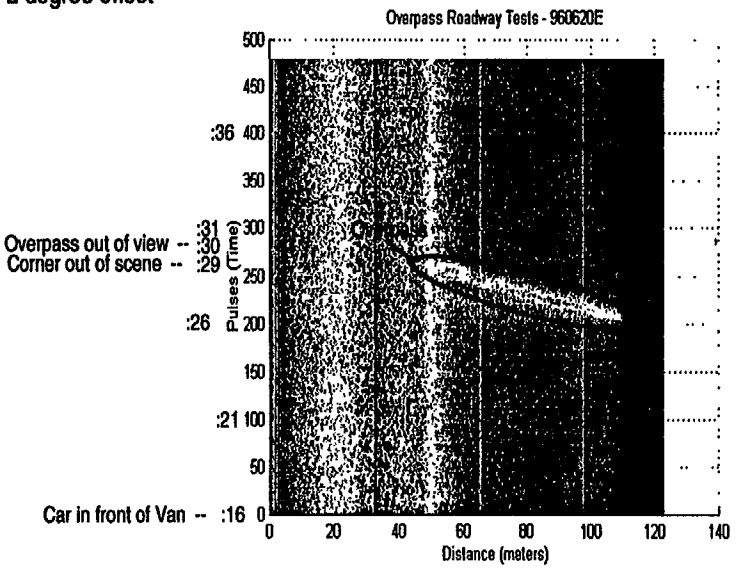

960620 - Overpass Roadway Tests

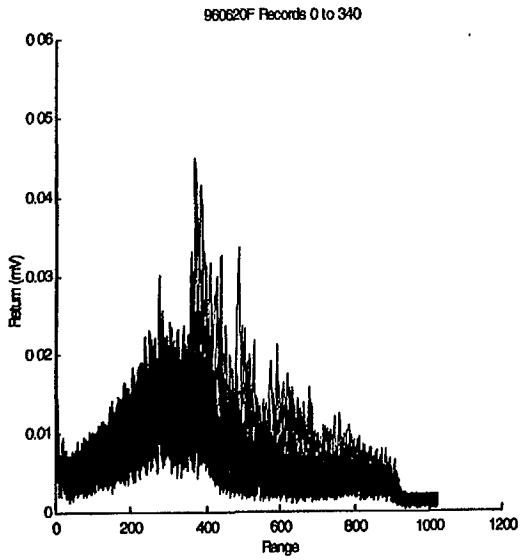

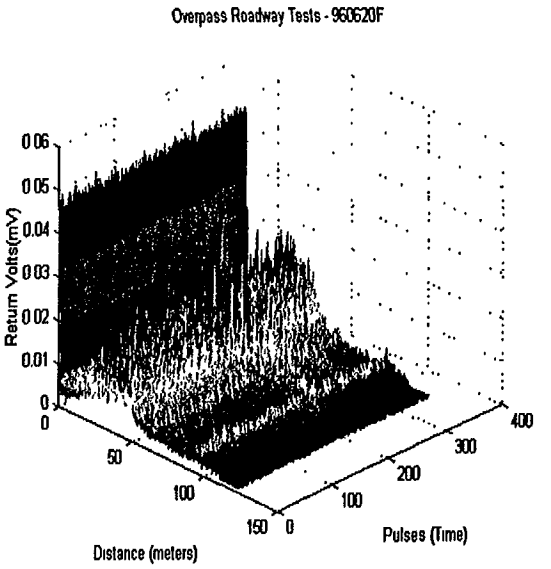

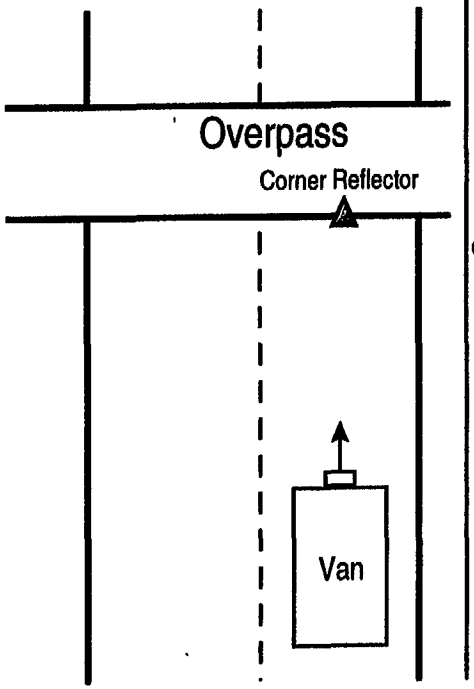

09:53:55 - Begin File
2 degree file

Overpass out of scene -- :07
Corner out of scene -- :06
:05

Minivan in center -- :02
of lane

:54:00

Minivan begins to cut -- :59
in front of Van

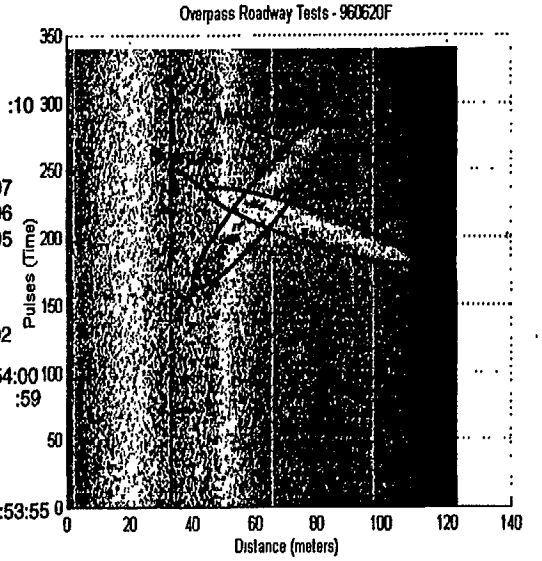

960620 - Overpass Roadway Tests

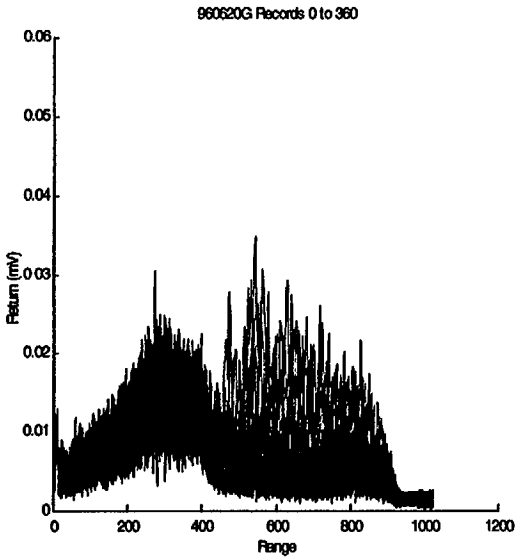

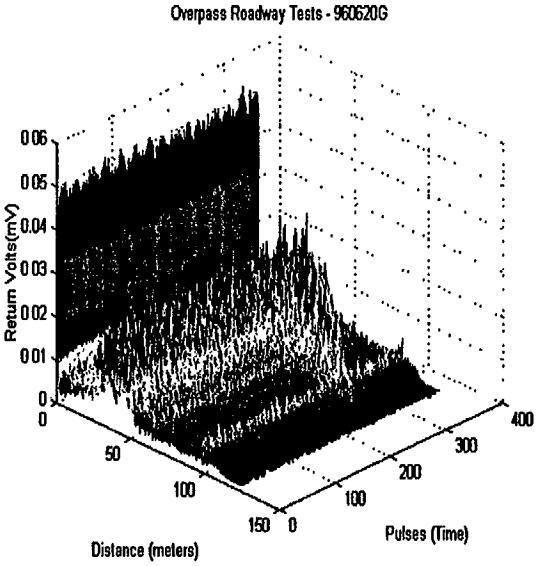

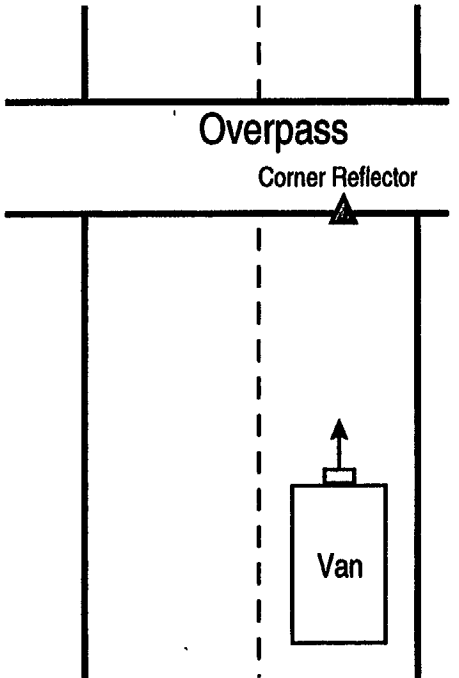

10:01:18 - Begin File
3 degree offset

Overpass out of scene --:32
Corner out of scene -- :31

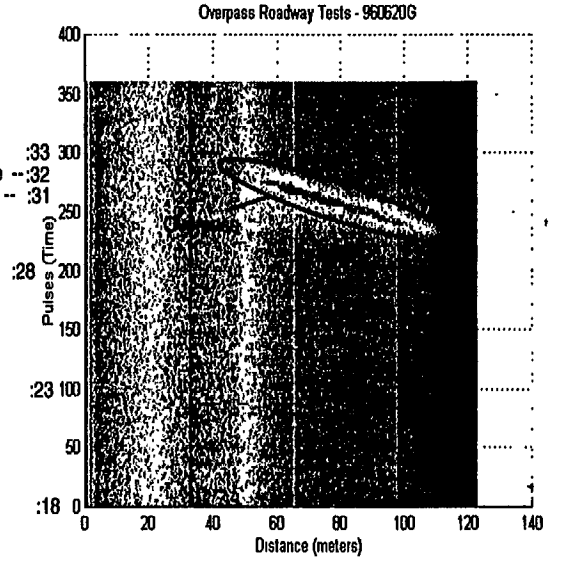

960620 - Overpass Roadway Tests

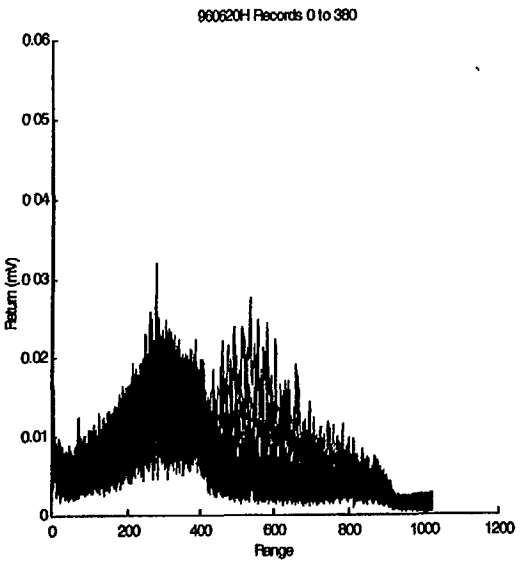

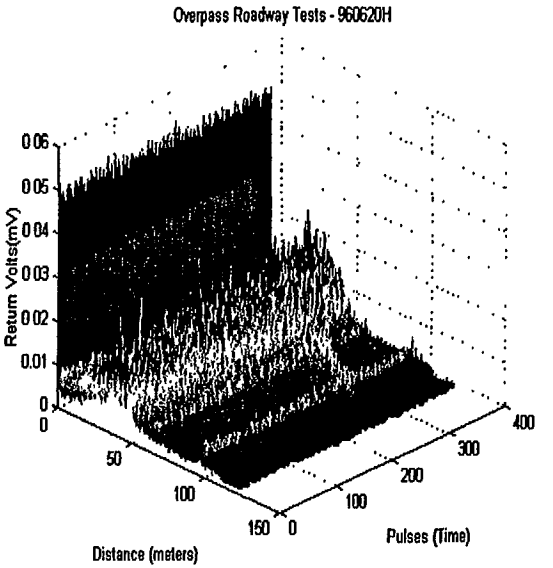

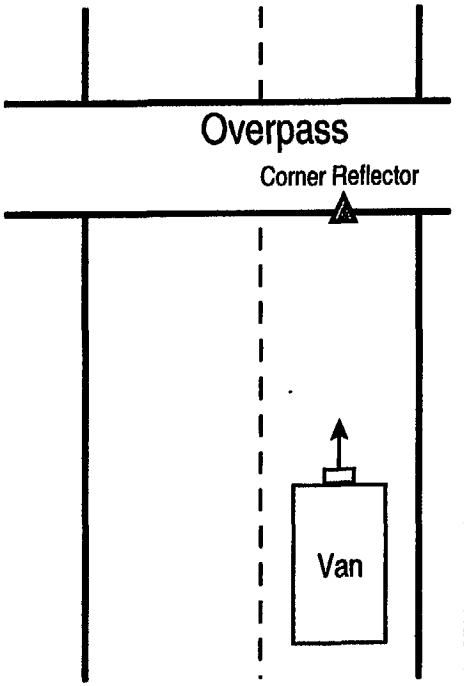

10:05:05 - Begin File
3 degree offset

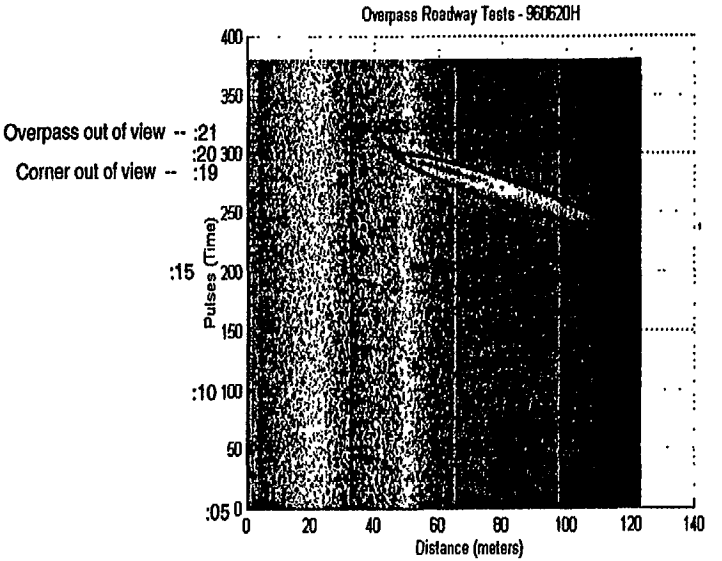

960620 - Overpass Roadway Tests

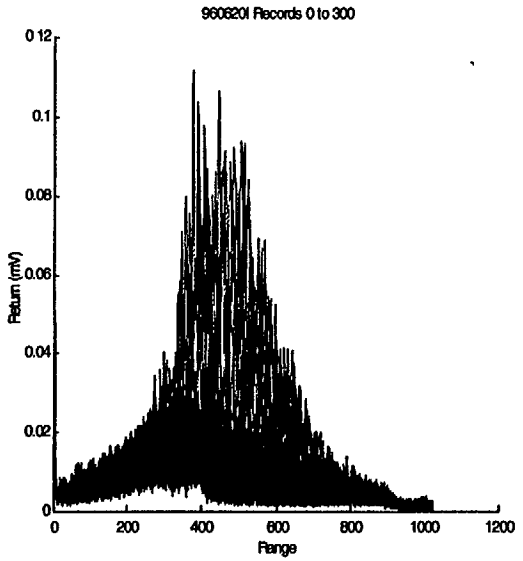

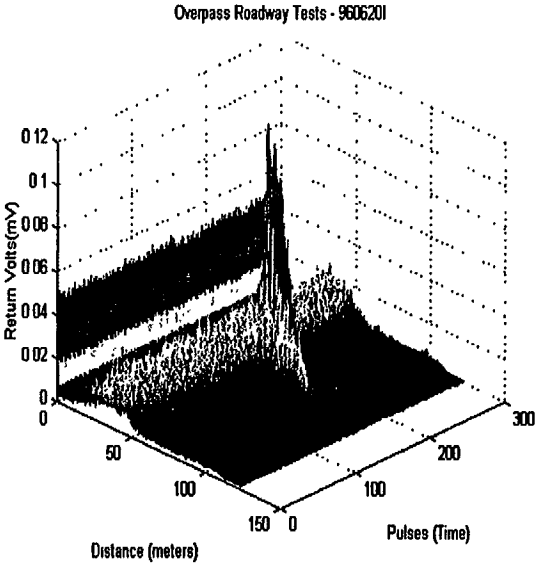

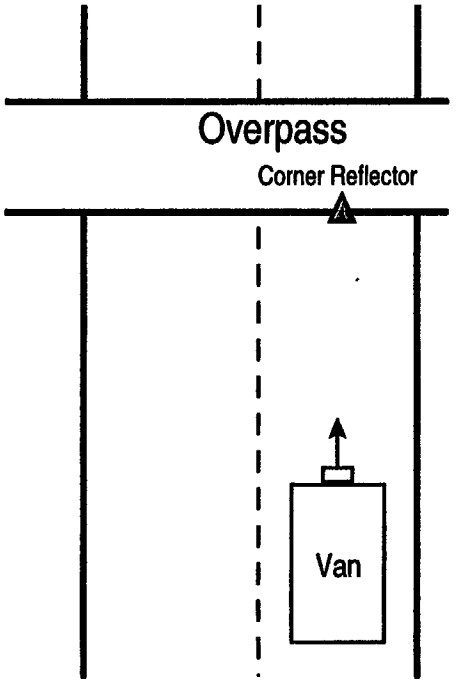

10:14:19 - Begin File
5 degree offset

Overpass out of scene -- :29
Corner out of scene -- :28

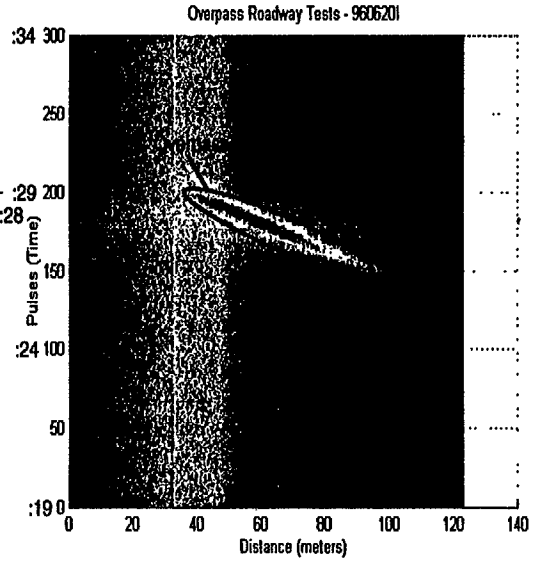

960620 - Overpass Roadway Tests

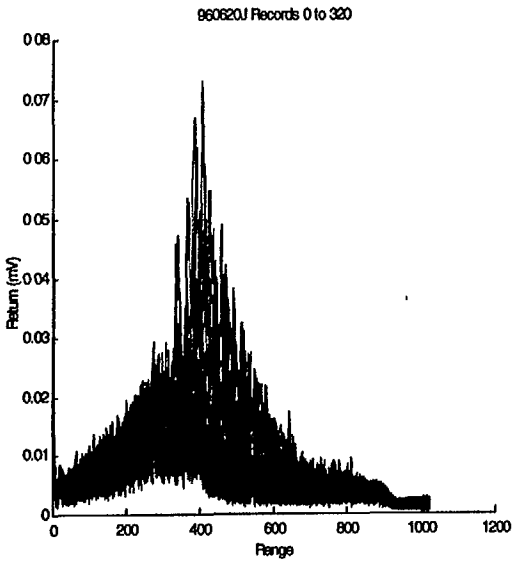

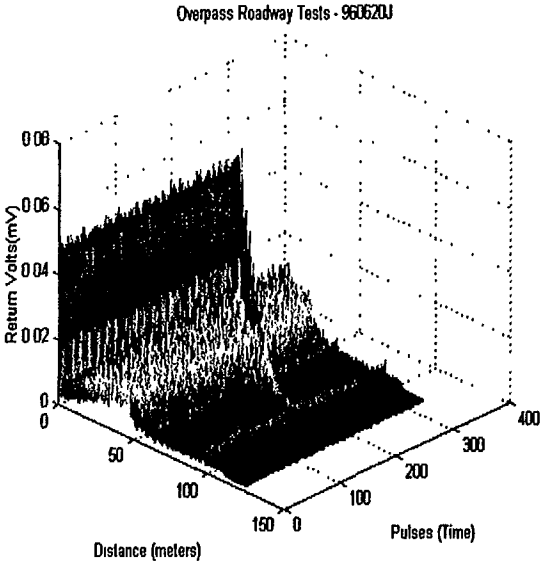

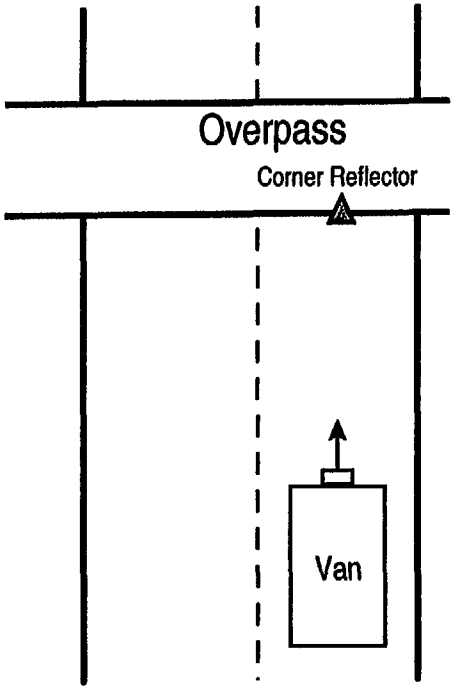

10:18:31 - Begin File
5 degree offset

Overpass out of scene - :41
Corner out of scene -- :40

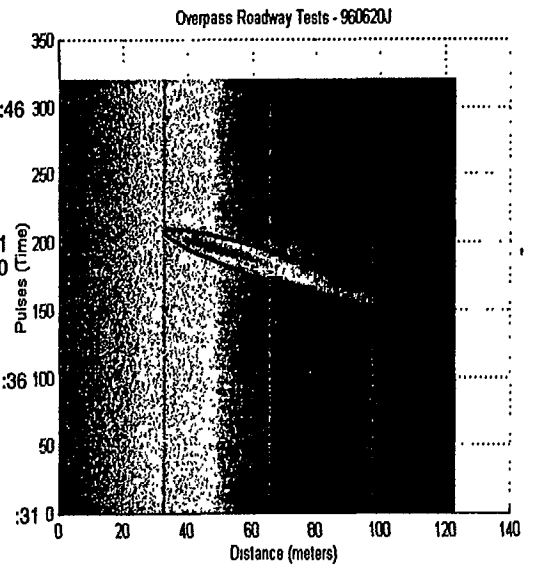

960620 - Overpass Roadway Tests

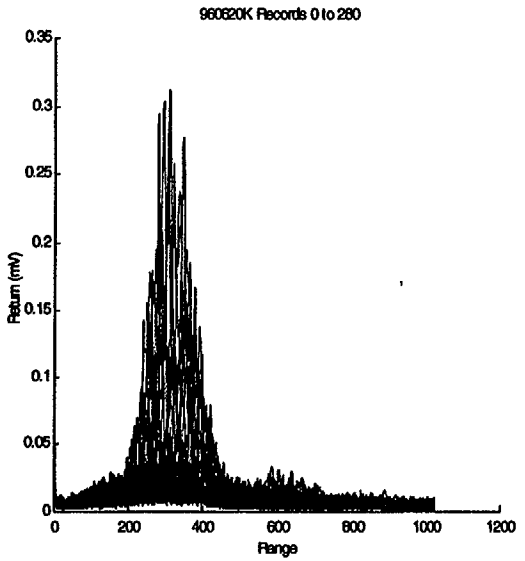

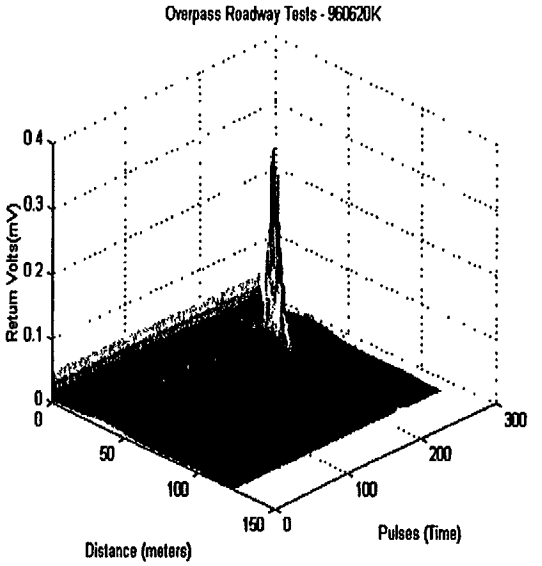

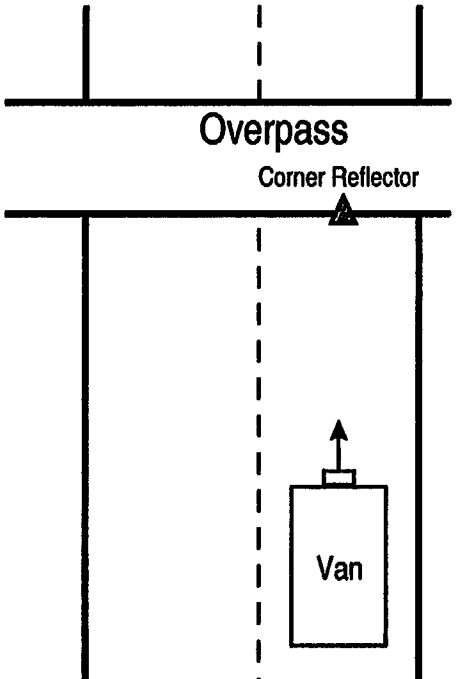

10:25:11 - Begin File
8 degree offset

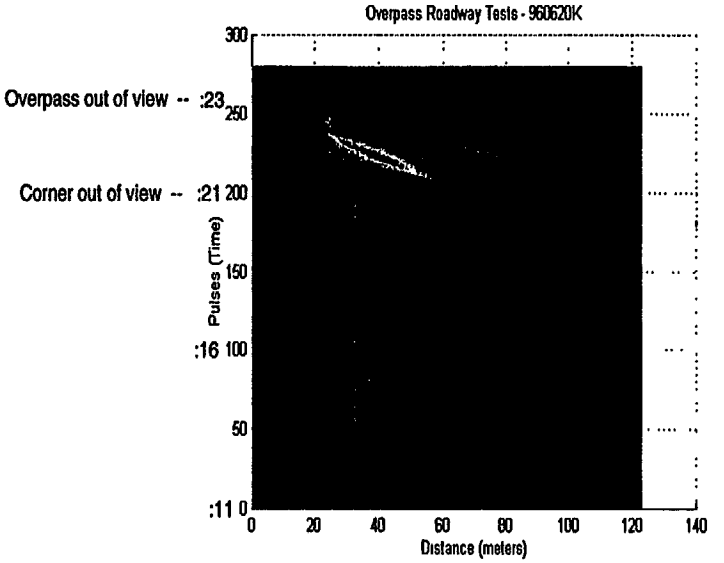

960620 - Overpass Roadway Tests

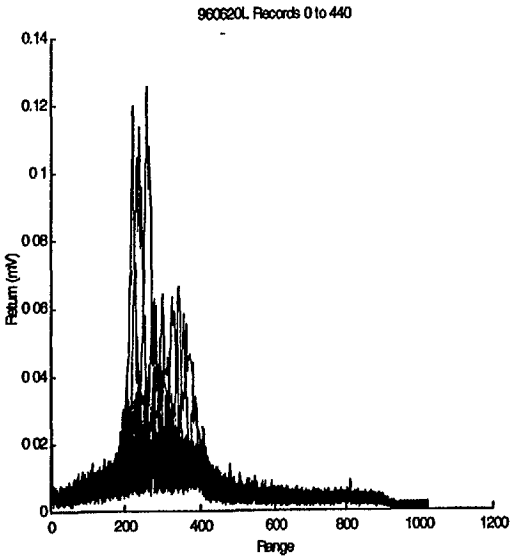

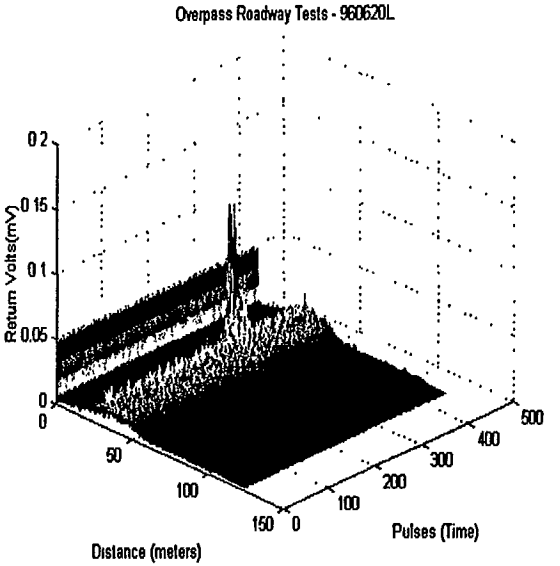

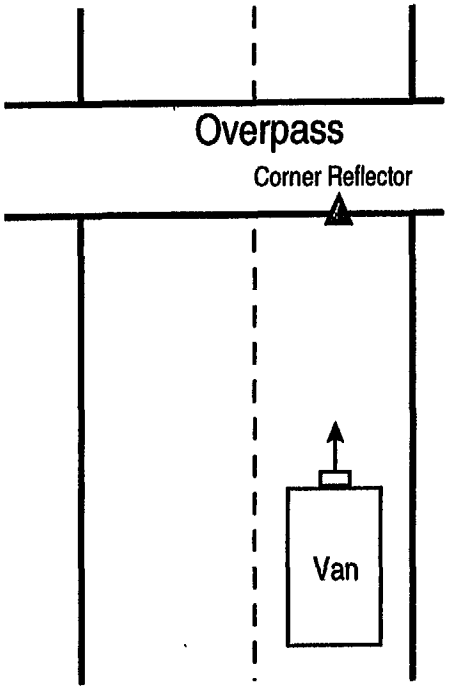

10:28:33 - Begin File
8 degree offset

Overpass out of view -- :47
Corner out of view -- :46

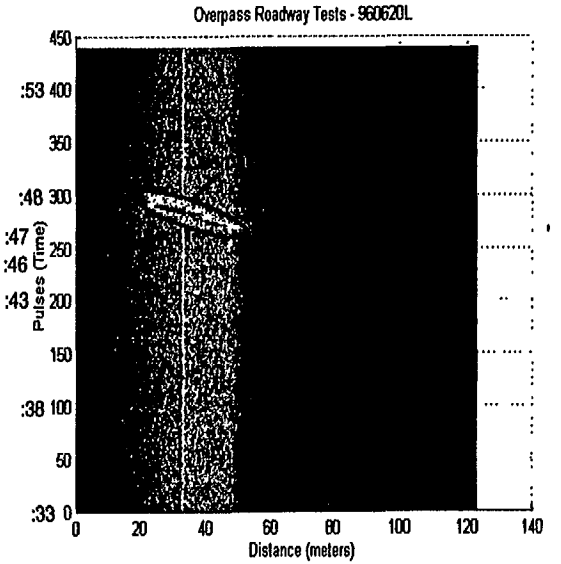

960620 - Overpass Roadway Tests

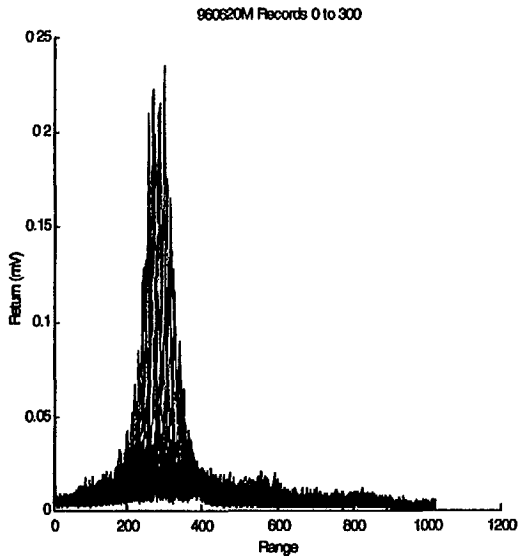

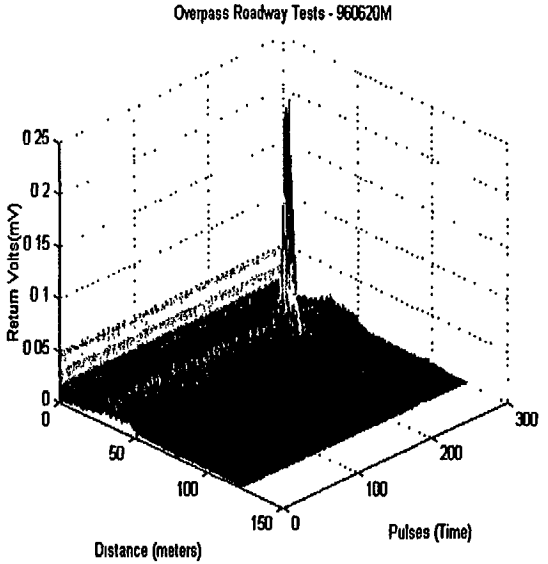

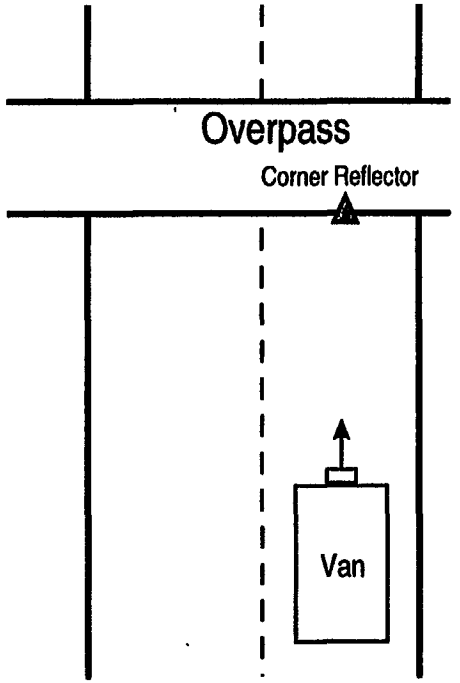

10:33:05 - Begin File
8 degree offset
* no corner present

Overpass out of view -- car cuts in

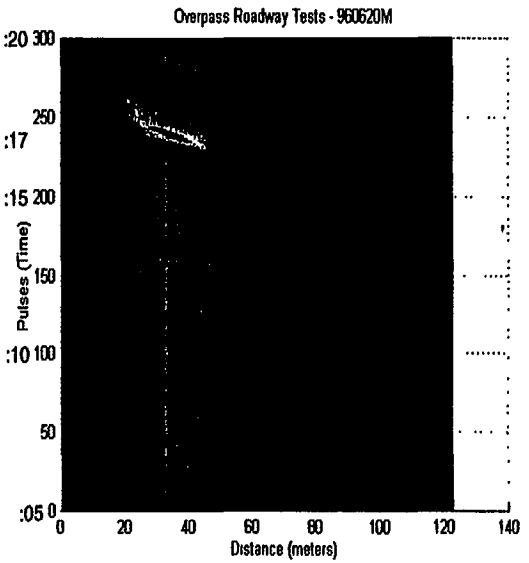

970301 - Roadway Backgrounds

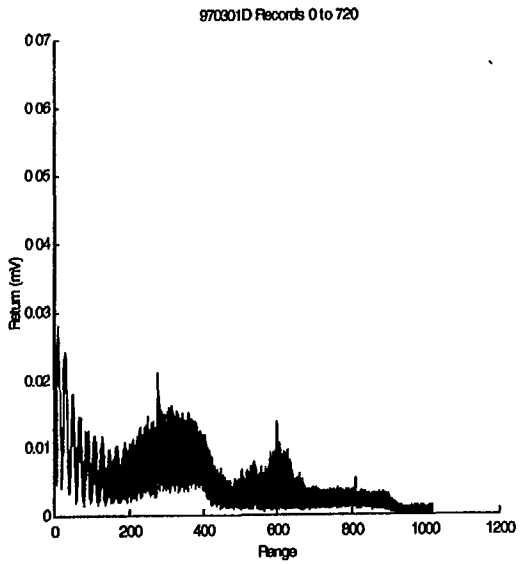

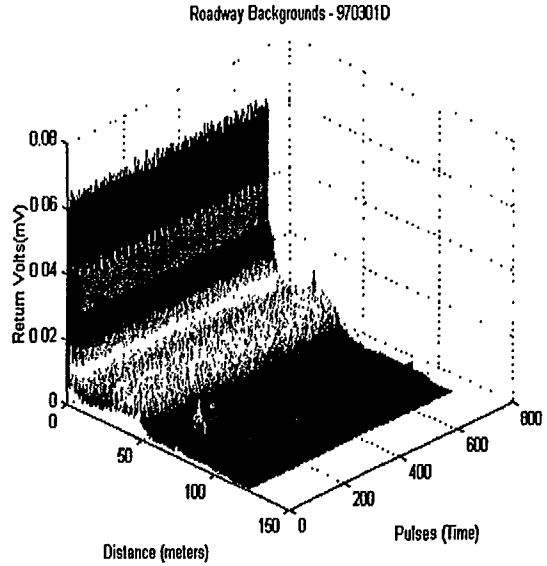

19:02:34 - Begin File

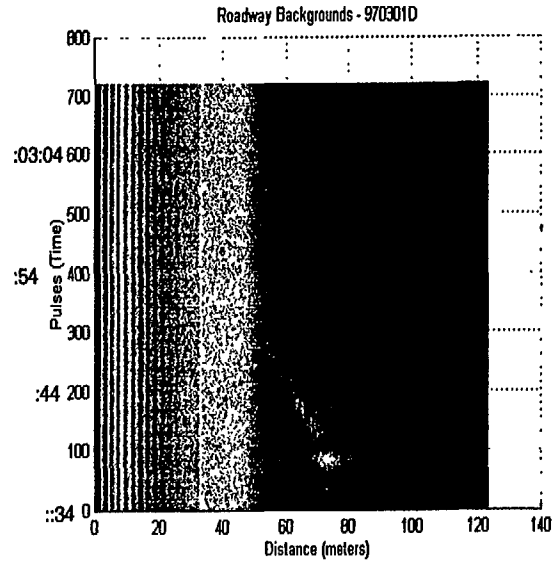

970301 - Roadway Backgrounds

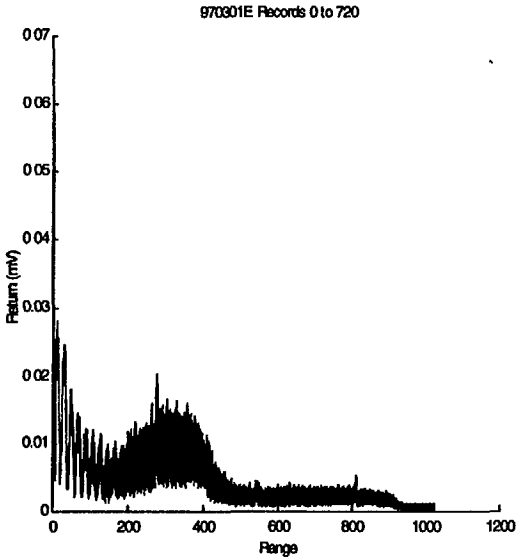

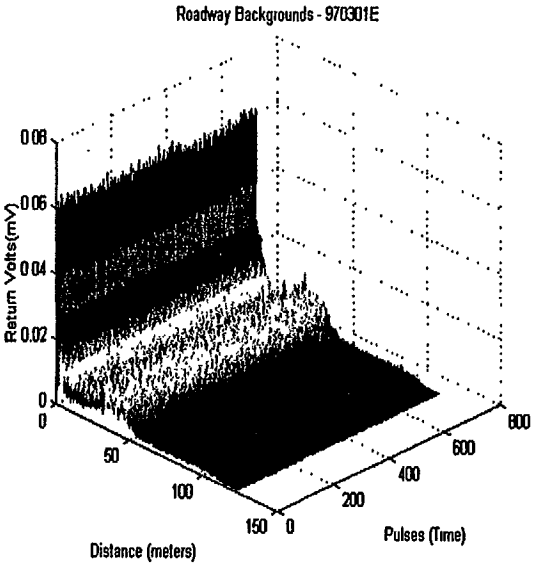

19:06:29 - Begin File

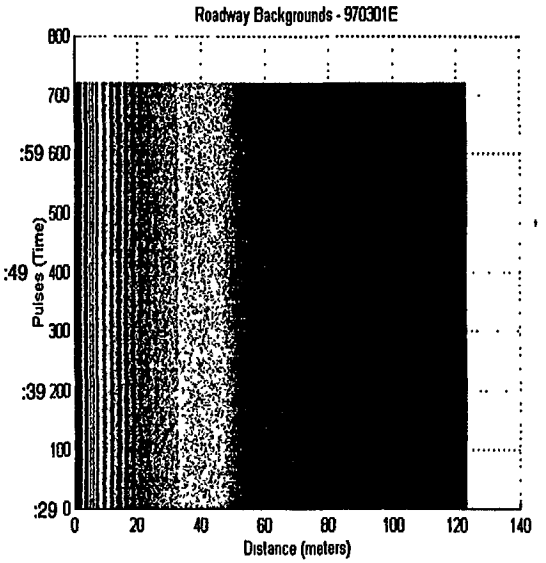

970303 - Open Roadway Tests

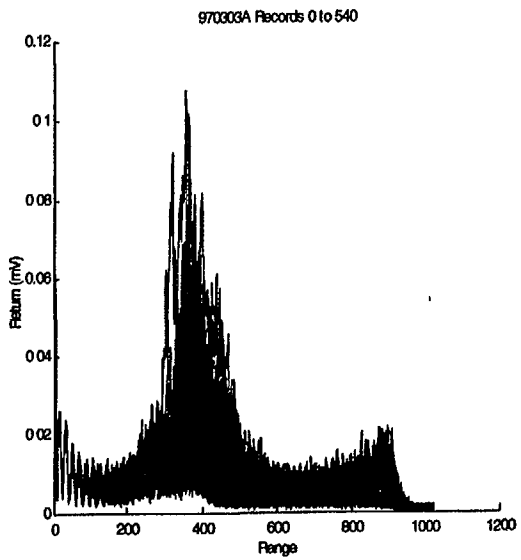

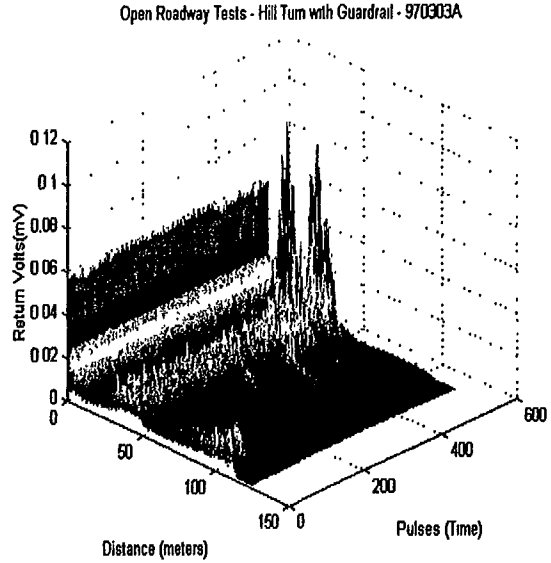

Hill & Turn with Guardrail
Two lane highway
Center Beam

19:22:45 - Begin File

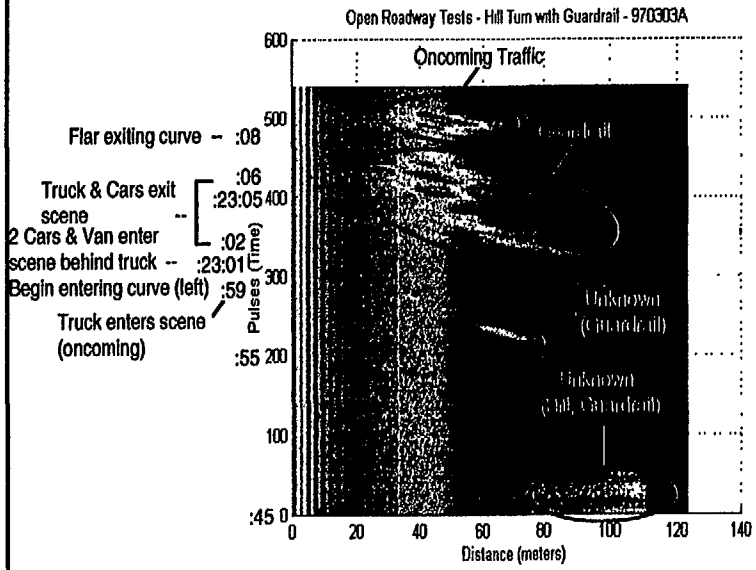

970303 - Open Roadway Tests

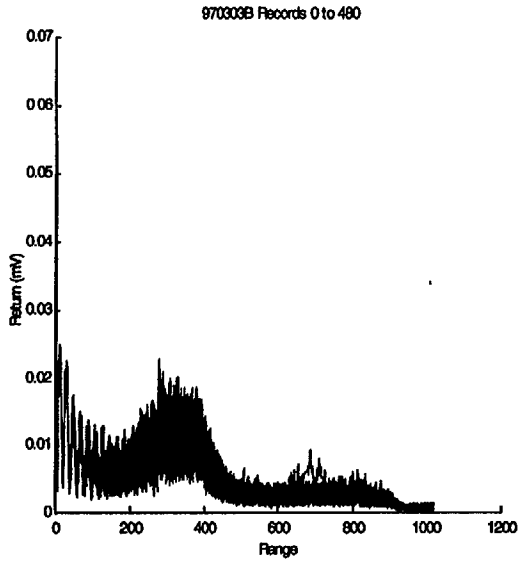

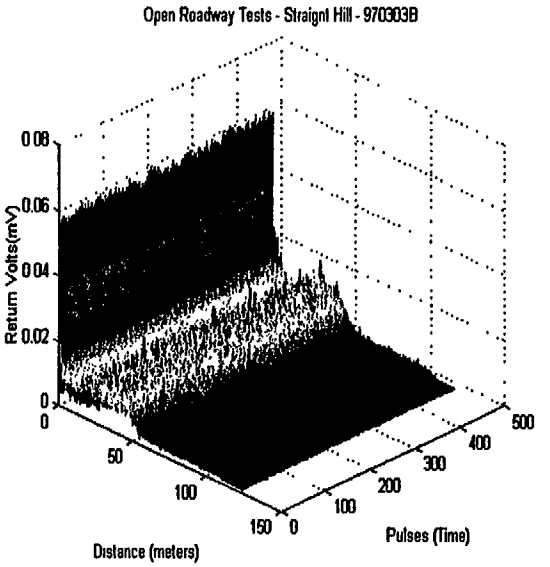

Straight Hill
Two Lane Highway
Center Beam

19:43:43 - Begin File

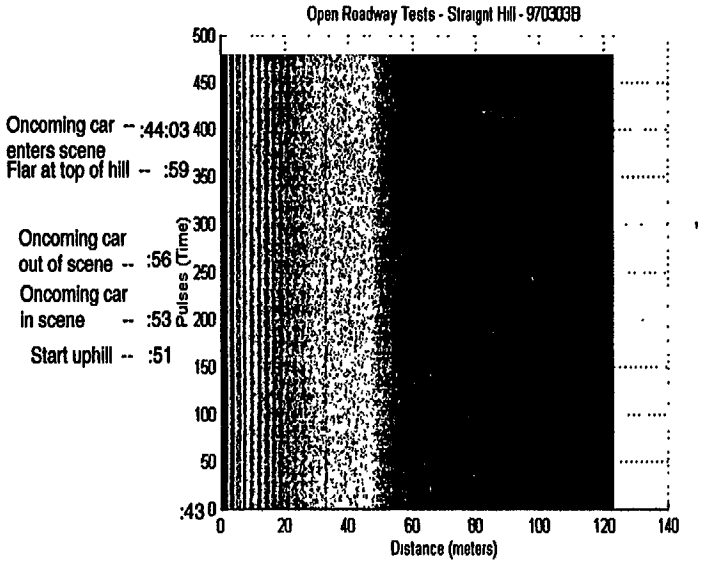

970303 - Open Roadway Tests

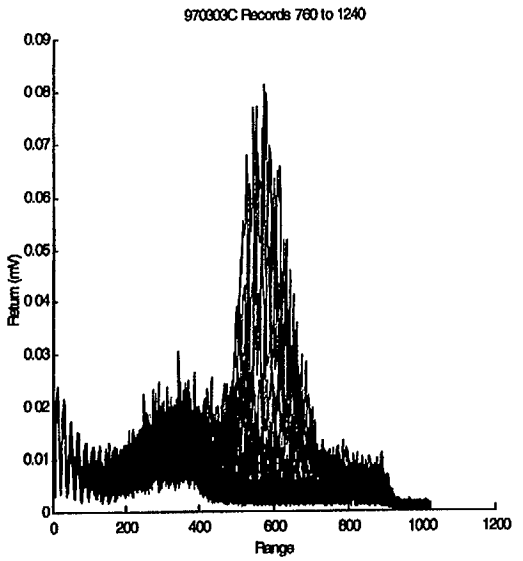

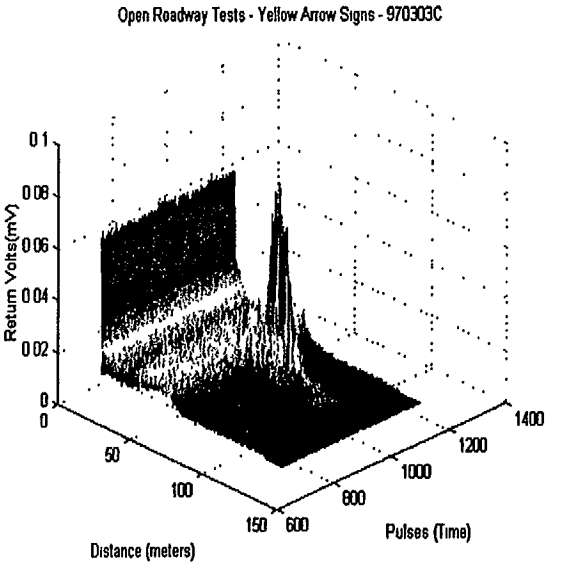

Yellow Arrow Signs on Curve
Two Lane Highway
Center Beam

19:59:27 - Begin File

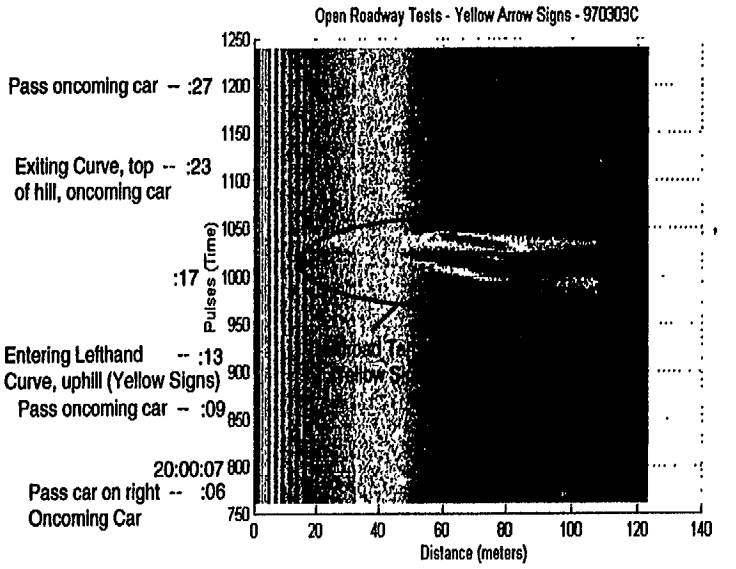

970303 - Open Roadway Tests

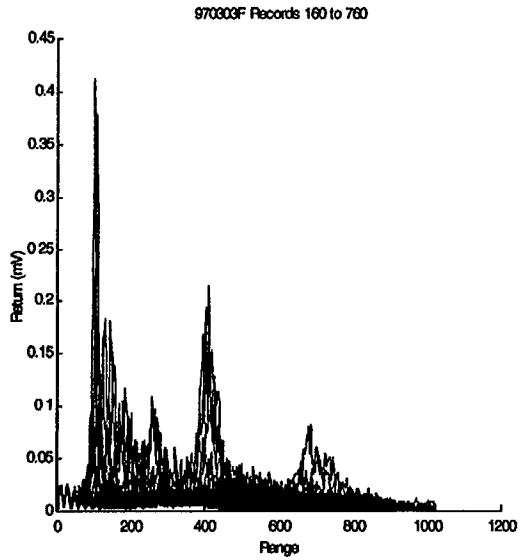

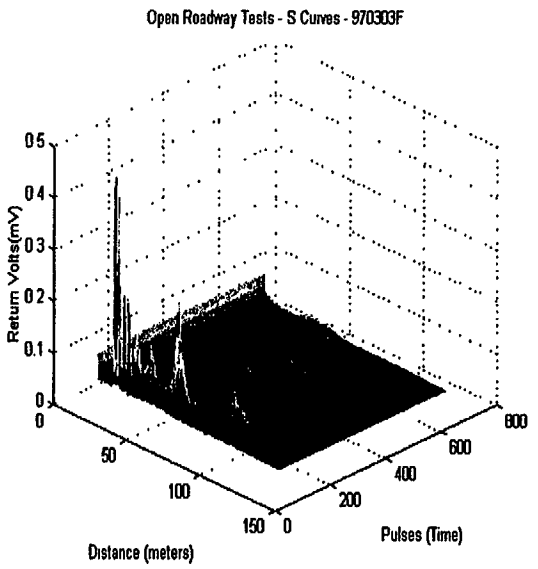

S Curves
Two Lane Highway
Center Beam

20:28:31 - Begin File

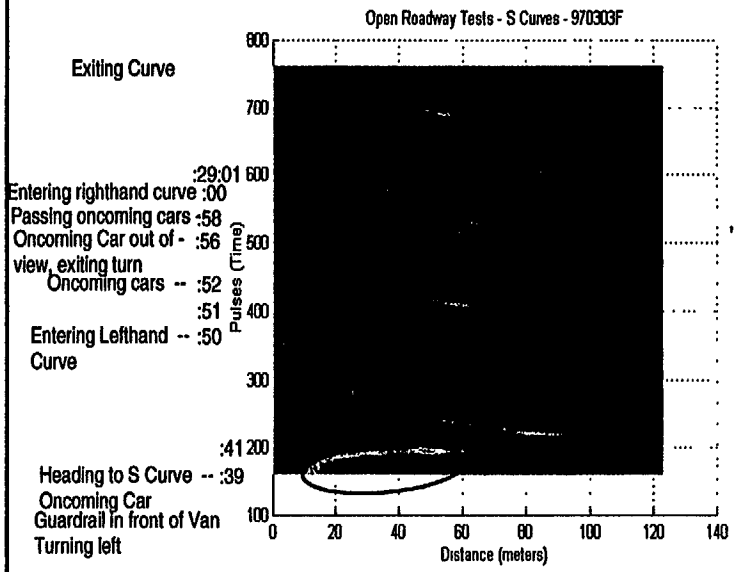

970303 - Open Roadway Tests

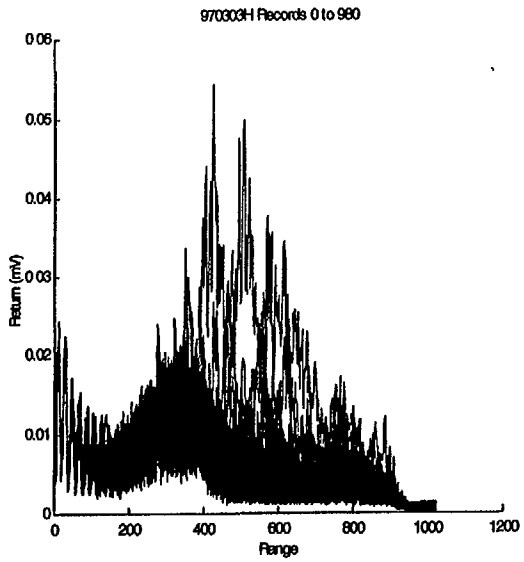

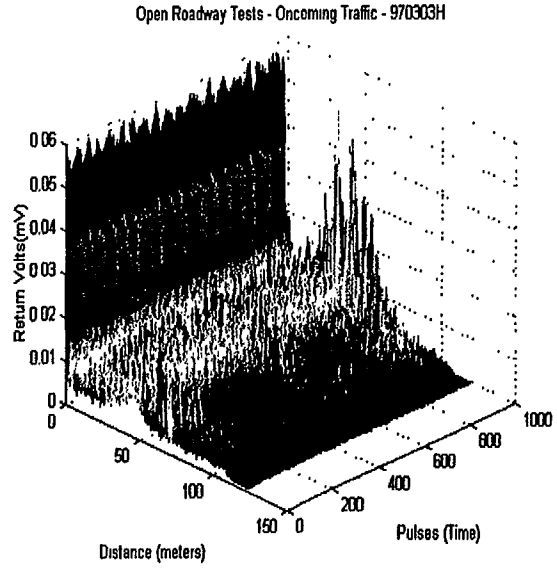

Oncoming Traffic
Two Lane Highway
Left Beam

20:58:38 - Begin File

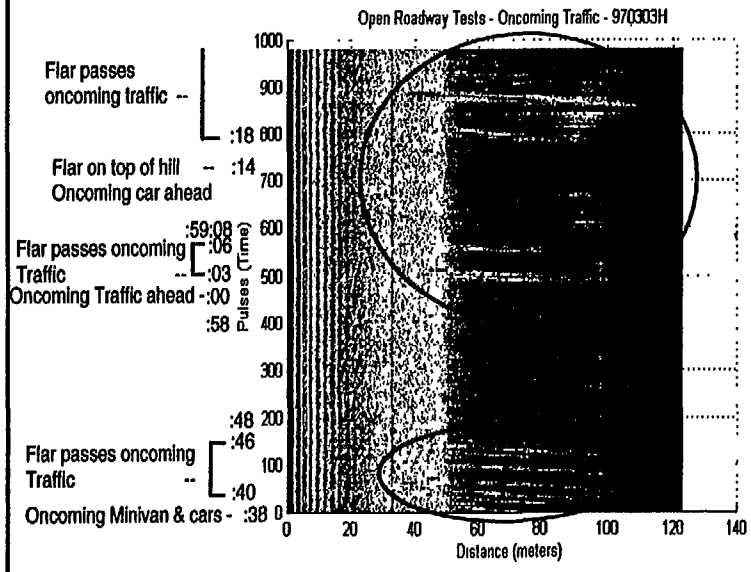

970303 - Open Roadway Tests

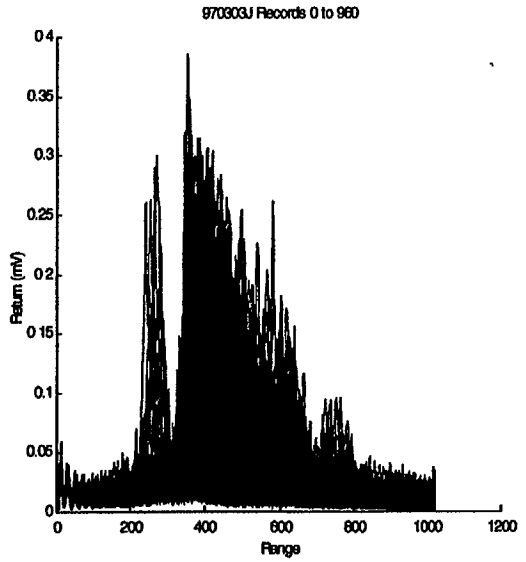

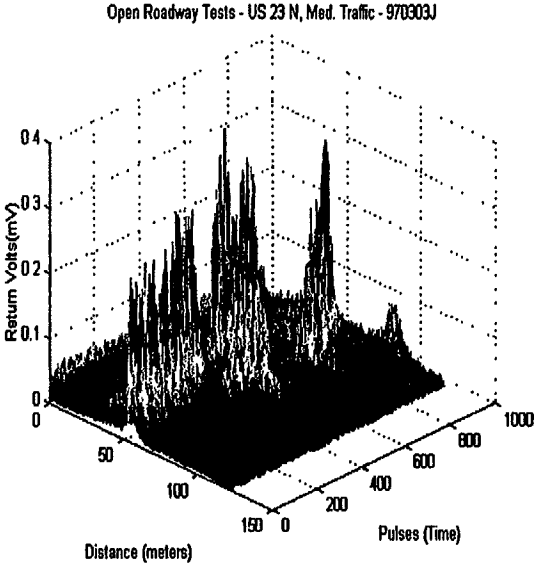

US 23 North - Medium Traffic
Divided Freeway
Center Beam

21:17:17 - Begin File

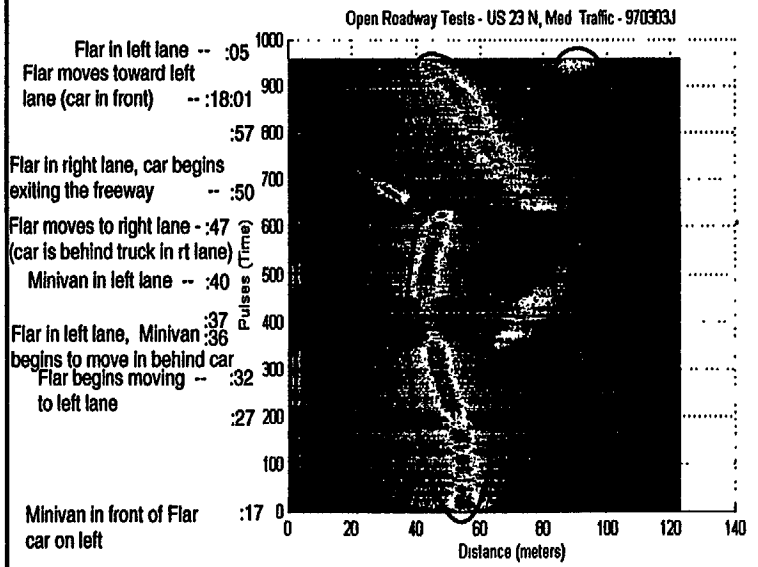

970303 - Open Roadway Tests

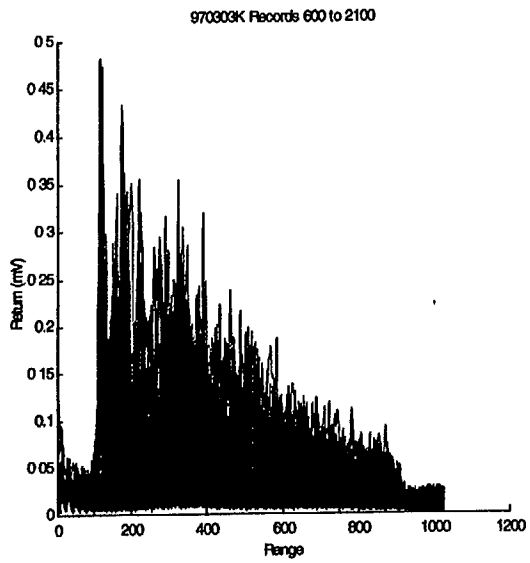

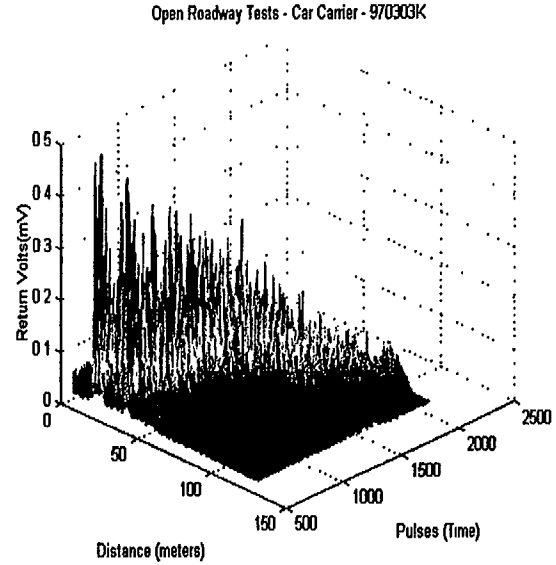

Car Carrier
Divided Freeway
Center Beam

21:31:15 - Begin File

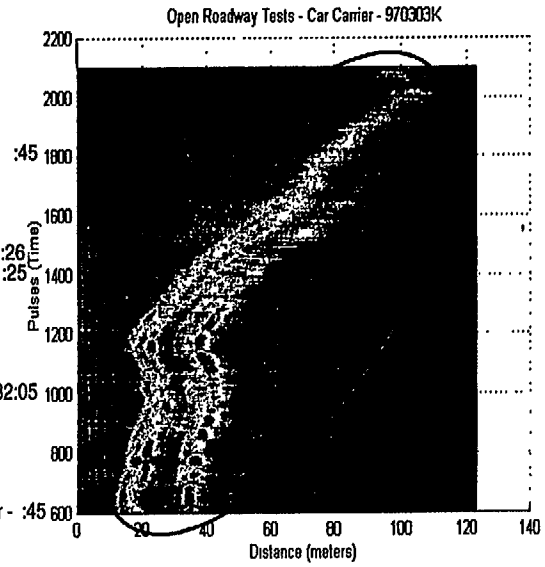

Carrier begins to change - :26
to left lane, flar changes :25
with carrier

:45

:32:05

Car Carrier in front of Flar - :45

970303 - Open Roadway Tests

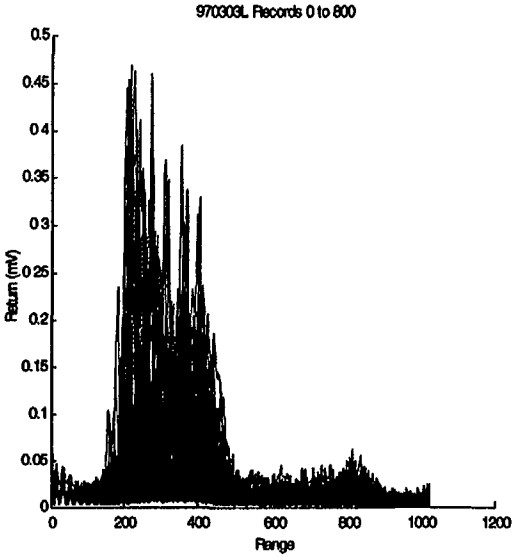

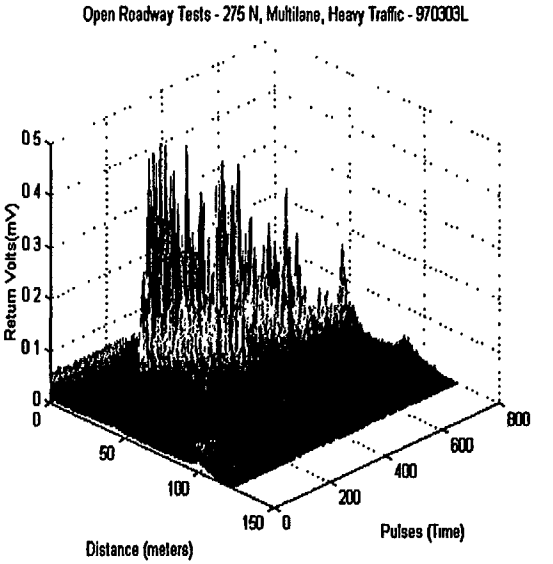

275 N, Multilane, Heavy Traffic
Divided Freeway
Center Beam

21:36:25 - Begin File